EXTRACTING SINGLE TARGET INFORMATION FROM A SIMPLE ECHO SOUNDER MOUNTED ON A DRIFTING FISH AGGREGATING DEVICE (FAD)

BY

ALBERT DAMPTEY-BOAKYE

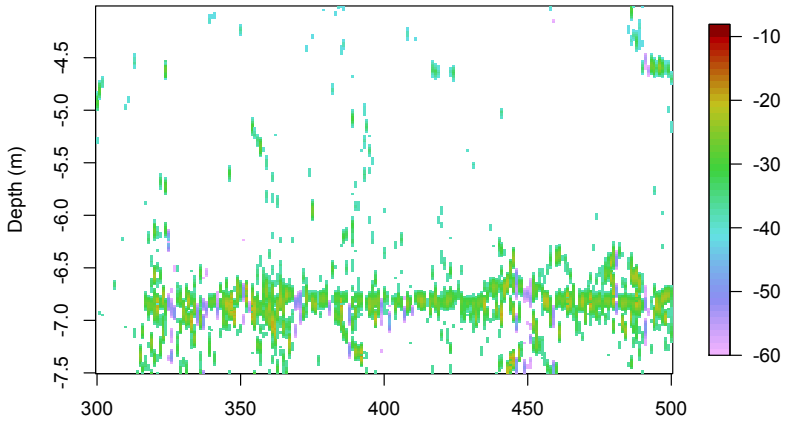

A THESIS SUBMITTED IN PARTIAL FULFILMENT OF THE REQUIREMENTS FOR THE DEGREE OF

MASTER OF PHILOSOPHY

IN FISHERIES BIOLOGY AND MANAGEMENT

DEPARTMENT OF BIOLOGY

UNIVERSITY OF BERGEN

JUNE 2015

THIS PAGE DELIBERATELY LEFT BLANK

DEDICATION

I dedicate this work Ms Susana Brobbey and Mr Arne Johannes Holmin (Post Doc candidate, IMR)

ACKNOWLEDGEMENTS

I am most grateful to the God, maker of heaven and earth for His indescribable love and mercy. I am also grateful to my supervisor, Professor Egil Ona, for his patience and careful tutorage. My regards also goes to Arne Holmin Johannes for allowing me to use his years of hard work in the R programming language for my analysis and also being there to assist even at odd times. My in-depth gratitude to my colleague and mentor, Rokas Kubulius (PhD), for all the time he took to explain the basics of fisheries acoustics and help me understand the concepts. My thanks also go to the Institute of Marine Research (IMR), especially to the Marine Ecosystem Group, Bergen, for allowing me to use their facilities. To Ms Susana Brobbey for carefully reading through my work.

Finally, thank you to Benjamin, Tina, Mary, Dennis, Diana, Stanley, Enoch, for being friends and family in this two years of study in Norway.

"Woy3 Nyame a, yede y3ho to woso a y´nim enguase da. Meda woase".

"In your light, we shall see light" (Psalm 36:9b).

ABSTRACT

Fish aggregating devices (FADs) are widely used by purse seiners in the tropical tuna fisheries. Many species of fish including juvenile tuna often associate with these FADS. There are global decline in tuna catch largely owing to the mortality of juvenile tuna often caught as bycatch. Therefore a direct method for sizing the fish prior to catching will be valuable information to mitigate juvenile fish mortality. Target strength is an indicator for how large the target is, as it is determined by the acoustic reflectivity of the fish. If the target possesses a swimbladder, it accounts for more than 90% of the echo energy of the target. This work sought to demonstrate the data collection capacity of simple echo sounders that can run on low power supply, and subsequently can be operated on batteries for an extended period of time. Acoustic data were collected using the SIMRAD ES10 single beam echo sounder at 200KHz and SIMRAD EK60 split beam echo sounder. Algorithms in the R statistical software were used for identifying and estimating target strength from single fish echoes. A linear relationship is assumed to exist between maximum TS of the dorsal aspect, and length of the fish in the form TS_{max} = "a" *log10 (L) – "b" (Nakken and Olsen, 1977). This is specific to a specie and frequency and has been estimated for many species at different frequencies. Therefore, using the TS – length of fish relationship, *TS = 20 * log 10 (L) - 68*, the lengths of fish were estimated. A way to transfer this information to the user in a reduced format is also discussed. This information may help in reducing bycatch leading to discard of non-target species and the catch of smaller sized tuna.

TABLE OF CONTENT

LIST OF FIGURES

LIST OF TABLES

CHAPTER ONE

INTRODUCTION

Tuna and tuna - like fish species have significant economic importance and serves as a source of food for many around the world (Majkowski, 2007). There are about forty different species spread over the Atlantic, Pacific, Indian Oceans and the Mediterranean Sea. The contributions of the various oceans to the total world catch varies from 70.5 % in the Pacific, 19.5 % in the Indian Ocean, with the Atlantic Ocean and the Mediterranean Sea yielding 10.0 % in 2010 (Majkowski, 2007). In the Atlantic Ocean, there are three principal tropical tuna species of economic importance, which are of relevance to the Ghanaian fishery. The Ghanaian tuna fishery is constituted mainly of bait boats and purse seine, which often undertake their operations around fish aggregating devices (FADs). The FADs are usually drifting along with beacons attached for geo-location and sometimes contains very simple echo sounders running on batteries. The simple outputs of these echo sounders are transferred over satellite and may only indicate the presence or absence of targets under the FAD.

1.1 Tuna

Tuna differs from other fish by their ability to retain metabolic heat in mainly the red muscles, brain, eyes and viscera (ICCAT, 2006). This is affected by the size and the developmental stage of the fish. Therefore adults are generally able to retain more heat (Brill. et al., 1999; Maury, 2005). Tuna has a unique swimming mode compared with other teleost (Graham and Dickson, 2004). They have high metabolic rate and frequency – modulated cardiac output. This enables them to undertake rapid swimming, reducing the temperature barrier and enabling them to move between higher latitudes and greater Ocean depths (Graham and Dickson, 2004).

The three principal species of economic value and catch weight in the tropical region are: the Skipjack tuna (*Katsuwonus pelamis* -Linnaeus 1758), Yellowfin tuna (*Thunnus albacares* - Bonnaterre 1788), and the Bigeye tuna (*Thunnus obesus* - Lowe, 1839). They contribute about 58.1 %, 26.8 %, and 8.2 % respectively to the total estimate of

the world tuna (Majkowski, 2010). These species are the most dominant and thus landed, traded, processed and consumed in most places in the world (Majkowski, 2010).

The skipjack tuna lives in open waters and is an epipelagic species. The maximum size in catches are often not larger than 80 cm, with maximum weight of 10 kg (ICCAT, 2006) and a life span of up to 12 years. Various studies have recorded different sizes at first maturity for different geographical areas ranging from 40 to 45 cm (Froese and Pauly, 2014). They inhabit water with a temperature range of 15 to 30 ^{o}C but are normally found in temperatures of about 20 to 30 ^{o}C (Forsbergh, 1980). They do not dive into temperatures more than 8 ^{o}C lower than the surface temperature. The minimum dissolved oxygen required is in the range of 3.0 to 3.5 ml L^{-1} at salinity of 5ppt (Barkley et al., 1978). Moreover, they spawn throughout the year in the tropical waters with the reproductive female spawning almost daily in several portions (Froese and Pauly, 2014). The eggs and larvae are pelagic and are often preyed on by other pelagic fishes (Collette and Nauen, 1983). Larvae are often found near the surface in offshore waters, schooling along with drifting objects, sharks, and whales. Skipjack tuna feed on crustaceans, cephalopods and mollusks (Kailola et al., 1993). They are highly migratory fish and do not possess a swimbladder. Skipjack tuna are on the IUCN red list of least concern with stable population trends (IUCN, 2014). See **figure 1** below for their geographical distribution and probability of occurrence in these areas.

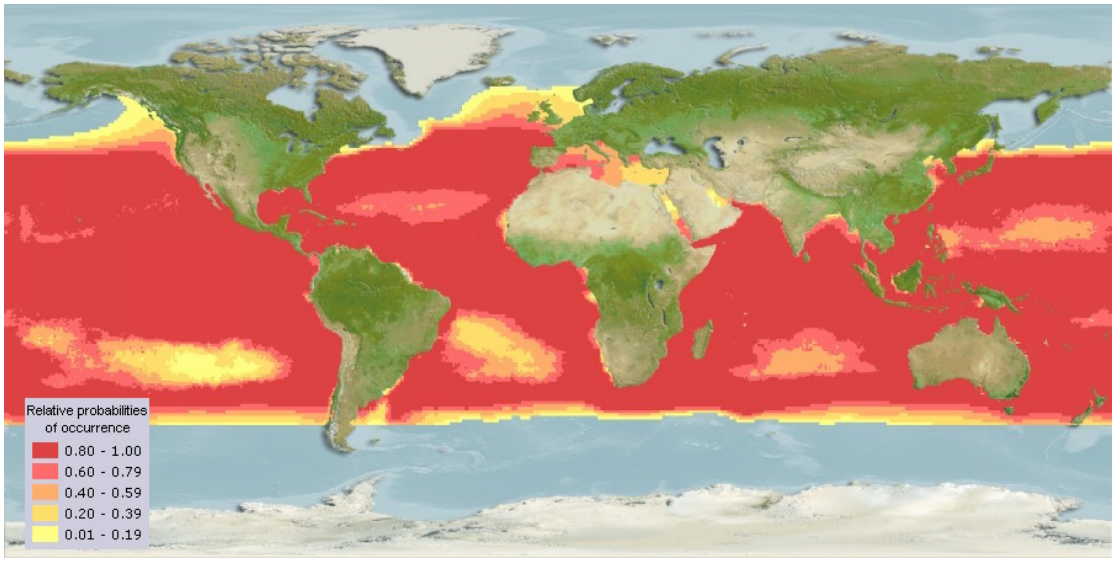

Figure 1. Skipjack tuna distribution and concentration. (Aquamaps, 2013b)

The yellowfin tuna is one of the three principal species of tuna. The largest yellowfin tuna recorded was 239 cm in fork length, though the most common maximum length of catches is 150 cm fork length (Collette and Nauen, 1983; IGFA, 2001). It grows up to a reported 9 years (Altman and Dittmer, 1962). Their geographical distribution is influenced by the temperature and oxygen variation in the water column. They are often restricted to the upper 100 meters with more than 2 ml/l concentration of oxygen due to the high sensitivity to low concentrations of oxygen (Sharp, 1978; Brill. and Holland, 1990). In areas with high concentration of oxygen however, the distribution is affected by changes in temperature of the water with depth (Brill. and Holland, 1990; Brill. et al., 1999). Yellowfin tunas spend most of their lives in waters with temperature of around 22 ^{o}C (Brill. et al., 1999). They are found in tropical and subtropical seas, but absent in the Mediterranean Sea (García et al., 1994), **(**See **figure 2** below).

The yellowfin tuna, like the skipjack tuna, are highly migratory and swim mostly in schools of similar size, either with same species or with other species. They are often associated with floating objects and frequently with porpoises (Collette and Nauen, 1983). They feed on other fishes, crustaceans and squids. It is the bright yellow central strip on either side of their body, and the shiny yellow rays with fine black edges that identifies them. They also have a swimbladder (ICCAT, 2006). The juveniles are mostly caught by surface fishing gear. They form schools with juveniles of other tropical tuna species in the coastal areas but move to deeper waters as adults (Miyake et al., 2004). It has been speculated that this movement could be as a result of the turbid waters of the coastal waters. Thus posing challenges in locating and capturing prey (Schaefer et al., 1963). The adults are however caught by both surface gears and long lines (Miyake et al., 2004). They are also listed on the IUCN red list of near threatened species with decreasing population trends (IUCN, 2014).

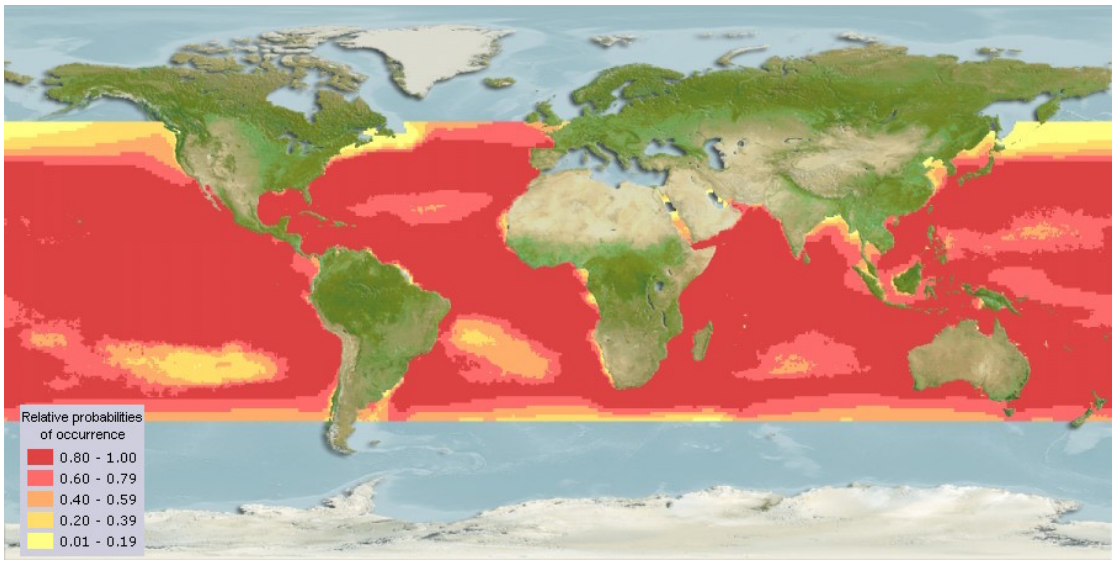

Figure 2. Yellowfin tuna distribution and concentration. (Aquamaps, 2013a)

Bigeye tuna are epipelagic and mesopelagic mostly living in open waters. It is reported to reach a maximum length of 250 cm (total length), although individuals between 40 to 180cm fork length are mostly caught (Collette and Nauen, 1983; ICCAT, 2006)**.** The maximum recorded weight is 210 kg with an estimated life span of up to 11 years (Stéquert and Marsac, 1989; Froese and Pauly, 2014). They are vertically distributed along temperature gradient between 13 to 29 ^{o}C, but the optimal range is from 17 to 22 ^{o}C (Maury, 2005). They have the ability to withstand lower oxygen concentrations than any other tuna species (Stéquert and Marsac, 1989). They can be found at depths with as low as 0.2 ml/l (Froese and Pauly, 2014). They are found at depths of up to 50 and 500 meters during the day and night respectively (Brill et al., 2005)**.**

They are normally caught together with the yellowfin tuna in surface gears. Moreover, the young of both species are very similar and therefore difficult to distinguish between them at this stage. Their characteristics vary between sizes of individuals and catch area (ICCAT, 2006). The juveniles form schools with other tuna species and are often associated with floating objects near the surface (Miyake et al., 2004). Adults swim in deeper waters and feed on other fishes, cephalopods and crustaceans (Collette and Nauen, 1983; Kailola et al., 1993). Bigeye tuna spawn at night, mostly few hours before midnight (Matsumoto et al., 2003). They spawn throughout the year from the coast of Brazil to the Gulf of Guinea at temperatures above 24 ^{o}C in locations rich in biological productivity (Rudomiotkina, 1983). They also possess swimbladder. They

are on the IUCN red list of vulnerable species with decreasing population trends (IUCN, 2014). See **figure 3** below for the geographical distribution and probability of occurrence of the bigeye tuna.

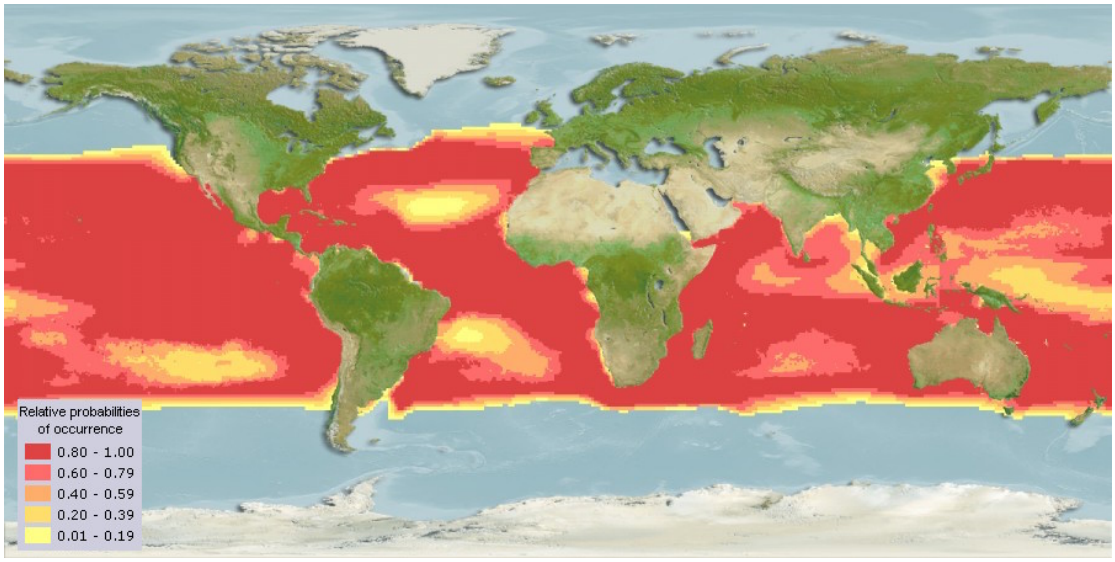

Figure 3. Bigeye tuna distribution and concentration. (Aquamaps, 2013c)

1.2 Tuna fisheries in Ghana

The Ghanaian tuna fishery started in 1962 by the Japanese with 5 bait boat vessels (Suzuki, 1979). The fishery depends on the three principal species and other minor tuna like species such as the frigate tuna (*Auxis thazard*) (ICCAT, 2014b). Ghana is one of the countries with the largest catches of the principal species of the tropical purse seine fisheries in the Atlantic Ocean along with Spain, France and Venezuela (ICCAT, 2008). The recent reports indicate a decline in the catches of the principal species from 69,852 tons in 2012 to 62,290 tons in 2013. The catch consist of 71 % skipjack tuna, 21 % yellowfin tuna, 4 % bigeye tuna, and 3 % other tuna-like species (ICCAT, 2014b).
Currently, there are 20 bait boats and 17 purse seine vessels reported to be operating in the Ghanaian Exclusive Economic Zone (ICCAT, 2014b). The use of FADs started with a few purse seine vessels in the early 1990s (Bannerman and Bard, 2001). However, both fleets now employ FADs in their operations with a reported 85 % of the total catch of the principal species being with use of FADs (ICCAT, 2014b). In Ghana, purse seine fishers collaborate with live bait boats often belonging to the same

company resulting in changes in the exploitation of tunas (Bannerman et al., 2005; ICCAT, 2006). In this collaboration, the catch is frozen on-board the purse seine and transferred to the bait boat. The number of purse seine vessels has increased constantly from two in 1996, eight in 1999, ten in 2005 and current number of seventeen (Bannerman and Bard, 2001; Bannerman et al., 2005; ICCAT, 2014b).

1.3 Sustainability and management

The tropical principal species of tuna, unlike the temperate species, have high fecundity, relatively short life span, wide geographic distribution and opportunistic behaviour. They are thus highly productive and react well to exploitation (Majkowski, 2010). There is increasing intensity of fish capacity as a result of the profitability of the tuna species. The current stock trends indicate that the species are being overexploited which could result in reduction in catches and other management concerns. The yellowfin and bigeye tunas are currently above the maximum sustainable yield in the Atlantic Ocean (Hallier and Gaertner, 2008). The sustainability of the tuna species requires management programs, for monitoring, international cooperation and capacity for fisheries research development, especially in developing countries (Hall and Roman, 2013).

Catches of yellowfin are often on free-swimming schools which are not in aggregation in the equatorial region (Fonteneau et al., 2000a). Unlike the yellowfin tuna, the bigeye are almost entirely caught under FADs with catches varying with seasons throughout the year, and mostly around the equator (Fonteneau et al., 2000a). Normally, they are not the main target of purse seine fleets but are often caught in association with skipjack and juvenile yellowfin. The catches of skipjack tuna with the purse seine started in the Gulf of Guinea in the 1960s by the French and Spanish fleets, which quickly replaced the pole and line boats (Miyake et al., 2004). The management of tuna in the Atlantic Ocean is under the International Commission for the Conservation of Atlantic Tuna (ICCAT). ICCAT coordinates research on tuna, develops science based-management device, and compiles statistics on tuna in the Atlantic Ocean. ICCAT recommended an annual total allowable catch of 85000 tons and 110000 tons for bigeye tuna and yellowfin tuna respectively for the year 2012. The quota were shared

between contracting parties and cooperating non-contracting parties (CPC) (ICCAT, 2014a). ICCAT also recommends a delimited area closure in the use of FADs each year, from 1st January to 28th February. During these periods, fishing activities under FADs, deployment or towing of FADs to areas outside the closed area are banned. This is aimed at protecting juvenile skipjack and yellowfin tuna (ICCAT, 2014a).

1.4 Tuna fishing

Skipjack tuna is the most dominant species caught under FADs with a notably high catch compared with catch of yellowfin and bigeye tuna (Fonteneau et al., 2000b). Tropical purse seine fishing in the Atlantic Ocean is mostly concentrated in the eastern part, with tropical tuna species being the main targets. The purse seine fleets mainly consist of Spanish and French vessels in the Atlantic Ocean.

1.4.1 Bait boats

Bait boats started in the Northern Atlantic in 1948 by the French fishers who introduced it from the Pacific Ocean. It quickly spread to other areas of the Atlantic in the 1950s and 1960s (ICCAT, 2006). It was later introduced to the eastern Atlantic for targeting yellowfin and bigeye tunas. It experienced its greatest growth in the gulf of Guinea mainly in Tema, Ghana, where it was started in early 1960s (Suzuki, 1979; ICCAT, 2006). The vessel searches for a school of free-swimming tuna. However since early 1990s, the Ghanaian fleets have been fishing with the aid of FADs (Bannerman and Bard, 2001). Ones a school of fish is located, live baits are thrown into the sea. A water spray pumping system splashes water from the side, hiding the shadow of the vessel and mimicking a large school of prey jumping around. Rods with hooks attached are thrown into the feeding school and retrieved. Then thrown in again and again until the whole school of fish is caught.

1.4.2 Purse seine

The tuna purse seine fishery is continuously developing in terms of size and techniques aided by modern technology. ICCAT records reveal increase in sizes of purse seine vessels in the Atlantic Ocean from 30 to 40 meters vessels to about 108 meters vessels (ICCAT, 2006). This has also resulted in the increase of the length and depth of the purse seine nets from 600 to 800 meters long, and 70 meters deep to the current large nets of up to 2000 meters long and 300 meters deep (See **figure 4** below) (ICCAT, 2006). Tropical tuna purse seine began in the 1950's and has developed since into the modern day purse seine boats. These boats have brine in cooling tanks for holding the catch at about -18 to -55 ^{o}C, and with high capacity storage tanks up to 3000 cubic meters. These vessel owners in some cases have supply vessels that refurbish the need of the purse seine vessels. This enhances productivity and prolong the days at sea, sometimes up to 3 months (Bromhead et al., 2003).

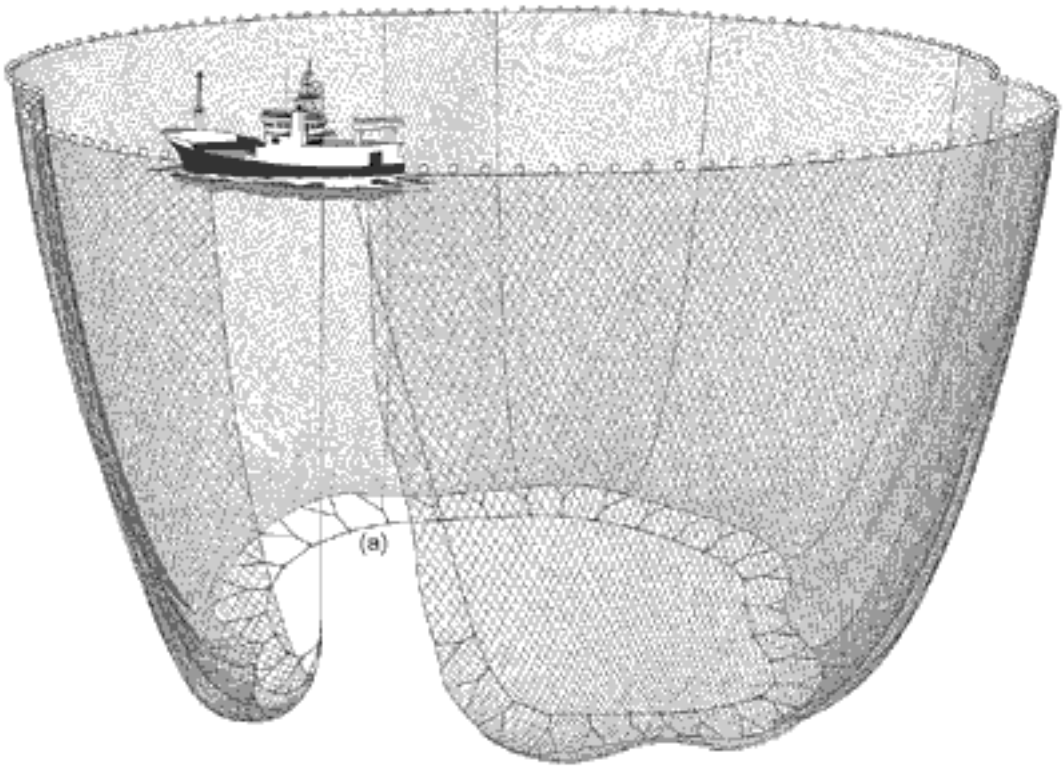

Figure 4. A purse seine during operation. (Eurocbc., 2015)

Purse seining is usually carried out during the day. Each cast is called a set, and depending on the tonnage of fish caught it could last between 2 to 3 hours. The purse seine fishery uses two main modes of fishing, either on free-swimming schools or under floating objects (Amandè et al., 2010). It has been observed that, up to about 90 % of sets in the purse seine fishery on FADs result in successful catches. Whereas successful catches on free-swimming schools is about 50 % (Fonteneau et al., 2000b). These vessels are often equipped with devices connected to communication networks with satellite information for easy location of schools under FADs. The vessels are often fitted with sonar, echo sounders and other detection systems (ICCAT, 2006). The FADs send information via the beacons attached to them on the presence or absence of fish aggregations, and other environmental data such as the salinity, temperature, etc. (ICCAT, 2006).

1.5 Fish aggregating devices (FADs)

Fish aggregating Devices (FADs) are floating objects, natural or man-made, anchored or drifting, which attract fish (Dagorn et al., 2013b; Gerald and Lopez, 2014). These FADs are either anchored near the coastline to enhance development of artisanal fisheries or are drifting FADs exploited by the purse seine fishery (Dagorn et al., 2013a). For thousands of years, fishers used different techniques for catching tuna (Gerald and Lopez, 2014). They observed that floating objects were points of aggregation for a number of species of marine life including dolphins, and bony fishes in all the oceans (Castro et al., 2001; Jaquemet et al., 2011). FADs were first used in the Mediterranean Sea and Malta in the 17th century. Fishers in the Philippines and Indonesia also used it in the early 1900's. It has been used by fishers in the Pacific since 1970 (Désurmont and Chapman, 2000).

In the mid 1980s, radio buoys and positioning devices were attached to the FADs for faster detection resulting in high development worldwide (Fonteneau et al., 2000b). These types of buoys attached to FADs have evolved, and the current echo sounder buoy uses multiple frequency transducers with satellite communication. This aids tracking and gives continuous information of the estimated amount of fish aggregated under the FADs (Lopez et al., 2014). Anchored FADs were first used as important tools

for the sustainability of small-scale artisanal fisheries in developing countries at low cost of fishing, and subsequently enhancing food security (Beverly et al., 2012). However, it is now used by both commercial and artisanal tuna fisheries to concentrate the fish, because the main tuna target in the tropical tuna fisheries, often associate with FADs (Gooding and Magnuson, 1967; Jaquemet et al., 2011; Gerald and Lopez, 2014; Lopez et al., 2014). The reasons for these associations are not known with certainty. However some hypothesis have been proposed to explain these aggregations; FADs are primarily being used by smaller fish as protection from bigger fish and predators. Also floating objects have concentrations of food supply such as zooplankton and sessile biota, this is termed as the "indicator FAD" (Gooding and Magnuson, 1967; Castro et al., 2001). These attract fish and are often indicators of productive areas. Moreover, tuna to increase encounter rate of isolated individuals and schools uses FADs. This is formulated as the "meeting point hypothesis" (Freon and Misund, 1999). These aggregations are not only found near the buoys on the surface but sometimes in deeper waters (Majkowski, 2010).

1.5.1 Design and impacts of FADs

The structural design and sizes of FADs are similar between fleets with significantly similar constituents for the construction, such as, the seine net, bamboo rafts, weight and coconut fronds (See **figure 5** below) (Fonteneau et al., 2000b). The typical drifting FAD design used in the Atlantic Ocean has bamboo rafts and some parts of a seine net hanging underneath. They often have coconut fronds tied in the seine nets providing places for smaller fishes to take refuge with a circular metallic weight hanging on the net as a drag. Moreover, buoys are attached for remote location of the FAD (Dagorn et al., 2013a). These radiolocation devices allow for real-time satellite feed (See **figure 6** below) (Fonteneau et al., 2000b). Skippers can understand the current pattern by using the movement of the FADs with the current and other satellite data information such as surface temperature, waves, etc., and this improves their searching pattern (Fonteneau et al., 2000b). The drifting FADs are designed with appending nets underneath it, length ranging from 15 to 100 meters differing from ocean to ocean. The deployment area is more important than the structural design in biomass concentration on the FAD (Gerald and Lopez, 2014). FADs are normally left in the water during the entire

lifetime of the FAD, which depends on the type of FAD and mode of construction (Morgan, 2011).

Figure 5. A typical new FAD. (Itano, 2012)

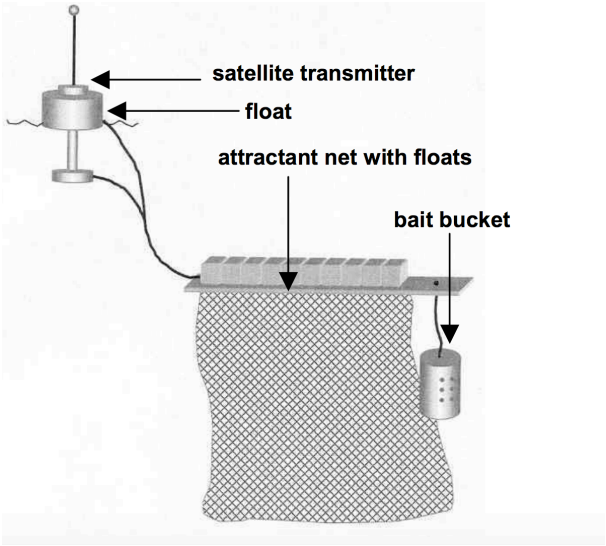

Figure 6. Schematic modern anchored drifting FAD. (Bromhead et al., 2003)

There are other species of commercial interest often aggregating under FADs along with the tuna species. It is reported that only a few species often account for over 95% of the total biomass of fish found under FADs. Some of these common species in the tropical pelagic include, dolphinfish, triggerfish, wahoo, rainbow runner, mackerel scad

and silky shark. The potential impacts of the use of FADs on the target stock, bycatch and potential effects on the biodiversity has been analysed by stakeholders in the tuna fishery (Dagorn et al., 2013b). There are growing concerns on the possible alteration of natural behaviour, age and size structure between free - swimming schools and those under FADs. Also, changes in migration pattern of tuna species resulting from the use of FADs is mentioned but too difficult to evaluate (Lopez et al., 2014).

The "Ecological trap hypothesis" has been proposed which indicates that tuna and associated species could be trapped in a network of FADs, and subsequently move along with the FADs into non-productive areas due to their strong associative behaviour. This could affect migratory paths and have resultant effects on their biological functions, such as growth and reproduction (Marsac et al., 2000). More than half of the major market tunas are fished around drifting FADs in the purse seine nets (ICCAT, 2012) . There is a rapid increase in the use of FADs in the major oceans around the world in the tuna fishery as opposed to free - swimming schools over the last few decades (Fonteneau et al., 2000b; ICCAT, 2012). The wide spread deployment of FADs could pose serious problems with regards to ecology, evolution and conservation of resources (Marsac et al., 2000). Globally, there are estimated between 47000 and 105000 FADS deployed each year, excluding those already in the water (Baske et al., 2012). In 2010, about 9000 FADs were recorded to have been deployed in the Atlantic Ocean (ICCAT, 2012).

1.6 Tuna as an acoustic target and relevance of swimbladder

The acoustic reflectivity of a fish must be known in order to interpret the echoes into fish abundance (Love, 1977; Warner et al., 2002; Simmonds and MacLennan, 2005). The acoustic reflectivity is expressed by the backscattering cross-section ($\boldsymbol{\sigma}$) or its logarithm, target strength (TS) (Simmonds and MacLennan, 2005). The behaviour of the fish such as the body orientation in the sound beam and its tilt angle whiles swimming are known to be important factors that affects the target strength of a fish species (Olsen, 1971). The echo amplitude is found to be strongly influenced by the absence or presence of the swimbladder (Foote, 1980). The relevance of the swimbladder of a fish in acoustic scattering has long been observed. It is estimated that

between 90 to 95% of the mean backscattering cross section of gadoids are contributed by the swimbladder alone (Foote, 1980). The acoustic backscattering is affected by the size and form of the swimbladder (Ona, 1990), thus the physical, biological and behaviour exhibited that affects the swimbladder influence the target strength of the fish species (Foote, 1980; Ona, 1990). **Figure 7** below shows a section of bigeye tuna and the swimbladder.

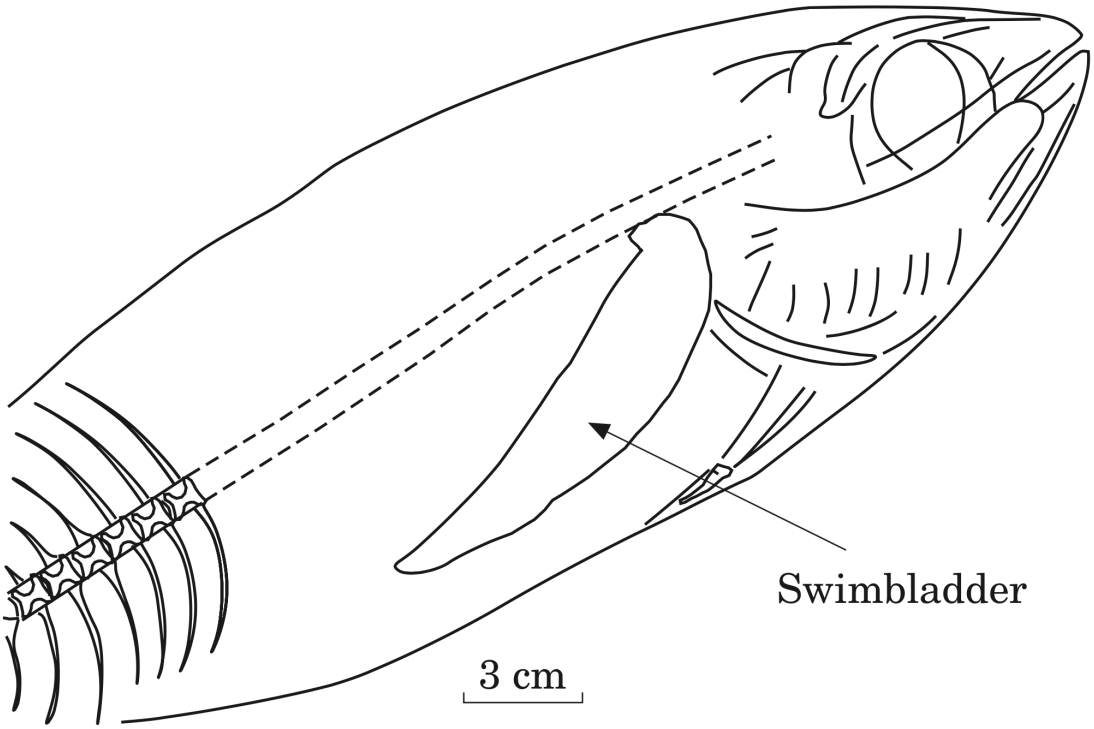

Figure 7. Longitudinal section of a 43cm bigeye tuna showing the swimbladder. (Bertrand et al., 1999)

Many species of bony fish possess gas bladder for several specific purposes. It may be used for sound production, respiration, hydrostatic activities among other important functions (Hall, 1924). The most important of these functions is for hydrostatic buoyancy, allowing the fish to maintain an equilibrium with the surrounding water at different pressures (Hall, 1924). The swimbladder is found between the alimentary canal and the vertebral column. There is a vascular area on a section of the surface of the bladder called the *rete mirabile* (Hall, 1924; Wittenberg, 1961). The *rete mirabile* is a complex counter - current heat exchange system which helps the fish to regulate body

heat (Majkowski and Goujon, 2000). The pressure of the gases in the swim-bladder must be maintained as pressure of the surrounding to obtain neutral buoyancy (Kuhn et al., 1963). This pressure can vary from 1atm at sea level to 100 atm at 1000 meters deep. The swimbladder are of two kinds: the physostomous, that is a bladder connected to the gut by a pneumatic duct, example; herring (*Clupea harengus*) and the physoclistous, in which the bladder is closed completely from the gut. Gaseous exchange is then achieved through secretion and reabsorption of gases to and from the blood. Examples of physoclists include, tuna, Atlantic cod *(Gadus morhua)*, saithe *(Pollachius virens),* and many others. The transport of gases into the swim bladder of fishes is through the combined action of the glandular epithelium in the *rete mirabile,* which acts as a large counter current system where the pressure of oxygen gradually builds up throughout the gland. The low-pressure side is the blood vessels outer side and the high-pressure side is inside the bladder (Wittenberg, 1961; Kuhn et al., 1963). In physoclists swimbladder, the release of pressure necessary when the fish moves to a more shallow depth is occurring in the oval area. A sphincter-controlled section of the swimbladder wall is covering a large blood capillary area in the dorsal part of the bladder. When it opens, gas flows into the blood capillary and is removed over the gills

1.7 Research motivation

FADs are widely used by the purse seiners in the tropical tuna fisheries to help them in their fishing operations (Lopez et al., 2010). The associated species in the tuna fisheries such as wahoo (*Acanthocybium solandri*), dolphinfish (*Coryphaena hyppurus*), triggerfish (*Canthidermis maculatus*), shark, small tuna and marine mammals are often caught as bycatch. The decline in catches around the world from the 1950s has been attributed to fishing pressure from increasing and advancing fishing technology (Lu et al., 2011). One of the major resulting effects is mortality of juvenile tuna often caught as bycatch (Lu et al., 2011). It has been found that a large proportion of the yellowfin tuna caught by purse seine using fish aggregating devices are immature (Lu et al., 2011). Therefore a quick and direct method of identifying species and to estimate the fish sizes present under the FADs through target strength measurement is needed This will help mitigate and reduce mortality of non-target species and juvenile tuna (Lu et al., 2011).

Tuna was not readily available for this particular study. Therefore, another fish of fairly large size and with similar acoustic backscattering properties as tuna was selected as a surrogate. Saithe *(Pollachius virens)* was selected. It is a widespread fish species in the North Atlantic and possesses a gas-filled swimbladder of considerable size, which accounts for most of the acoustic backscatter from a fish. Like tuna, Saithe does not form very dense schools and thus provide good conditions for single acoustic target detection. Cod (*Gadus morhua*) was also selected for the split beam data analysis. Like the saithe, cod is a fairly large size and data readily available for analysis from a cod survey.

This thesis sought to demonstrate the data collection capacity of simple echo sounders that run on low power supply. This can therefore be operated on batteries for an extended period of time. If successful, such information can improve the remote acoustic information from the buoys using target strength to distinguish between fish sizes below the FAD. This information may help in reducing bycatch and discard of unwanted species and catch of smaller sized tuna.

The specific objectives of this project were:

1. Evaluate, the possibility of extracting target strength information from a very simple echo sounder
2. Investigate and compare target strength from standard scientific split beam system and simple single beam echo sounders.
3. Evaluate how accurately fish size may be estimated from single echo analysis by the simple echo sounder.
4. Propose a data format for sending this information as a single text string over the existing satellite link between the FAD and the vessel.

CHAPTER TWO

MATERIALS AND METHODS

2.1 Study Site

The data used for single beam analyses were collected close to the fish farming plant at the Aquaculture Station of the Institute of Marine Research (IMR), Austevoll. Austevoll is an Island located south of Bergen. It is located on latitude 60.09 N and longitude 5.27 E. The data collection was carried out from 4th to 6th December 2014 during which time schools of saithe were passing through the surrounding waters. The saithe were identified using video cameras lowered about 5 meters below the water surface and about 3 meters away from the transducer. This is to ensure that the camera does not fall within the beam pattern. Saithe were used, as surrogates for tuna since the presence of swim bladder and large sizes are favourable for single target measurements. The Split beam data were collected around the Lofoten Islands, Norway. The data collection was carried out with the Norwegian research vessel "G. O. Sars" as part of routine cod survey. Biological samples were collected with trawl and species identified. Lofoten islands are located on the North - western coast of Norway. The sample site is located at Latitude 67.85^{o} N, longitude 13.25 E. See **figure 8** below showing the data collection sites.

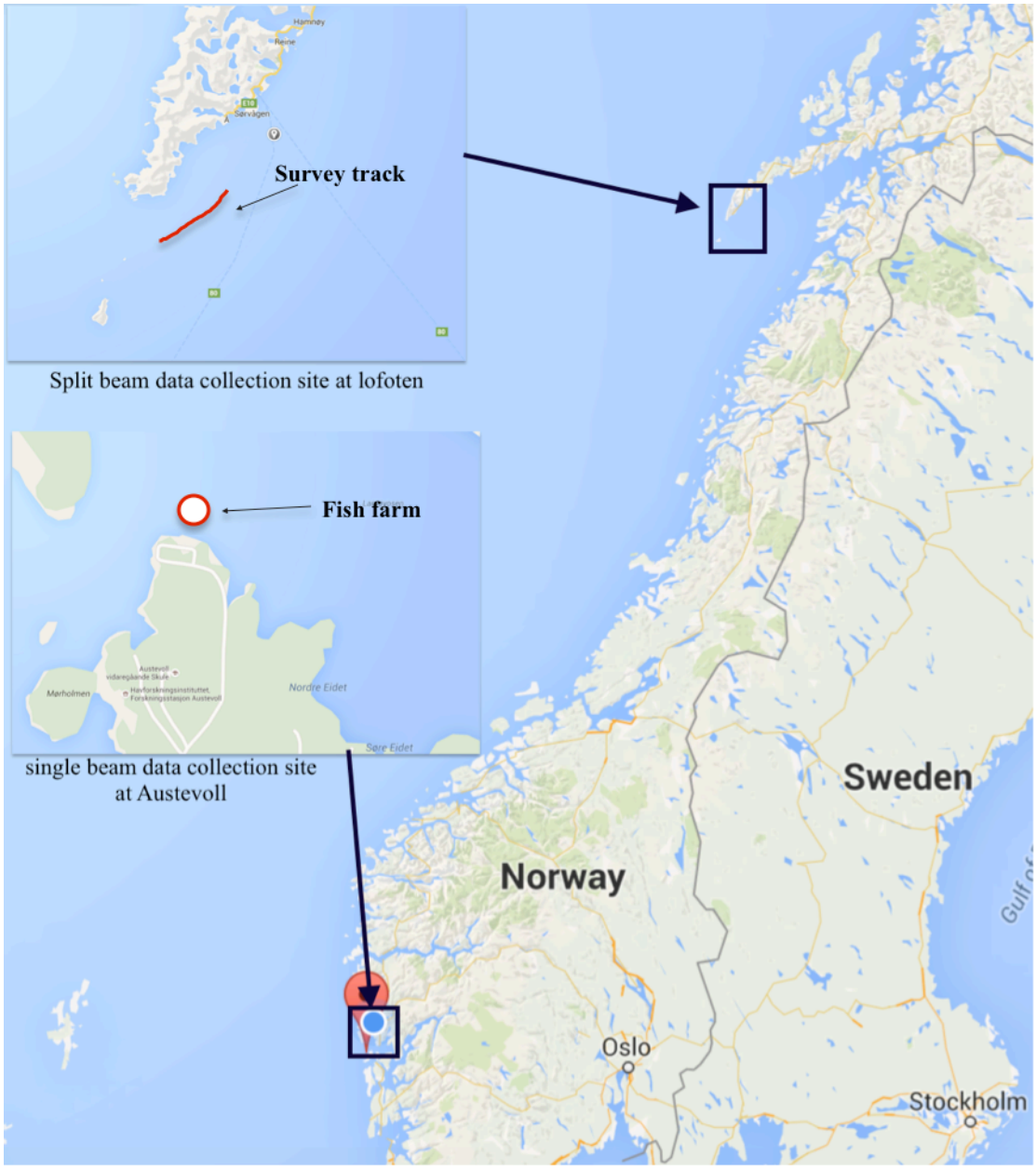

Figure 8. A map indicating the data collection sites of both split beam and single beam. (GoogleMap, 2015)

2.2 Experimental design and data collection

2.2.1 Single beam data

The single beam analysis data were collected with a simple SIMRAD ES10 echo sounder of 200 kHz and a transducer half-power beam angle of 28 ^{0}. The pulse duration was 0.33 ms and a sample rate of 21 μs. A total of 1500 TVG (20 log TVG)

compensated samples are delivered for every ping. This simple echo sounder was selected because it offers an opportunity to be placed under FADs due to the low power demands and thus its ability to run on battery lasting for a long period of time.
The data range of detection of this echo sounder is mathematically expressed as

Raw data sample interval (sample range in water)

$$= \frac{1}{\mathrm{f}} * \frac{\mathrm{c}}{2} * \text{Divisor} \qquad (1)$$

The divisor is an internal parameter between 4 and 32 and is controlled by the sample rate. The sample rate has a corresponding divisor in the multiples of 4 through to 32. The raw data in Austevoll was recorded at an internal parameter setting of 4.
The sample rate is a multiple of 21 μs to 168 μs. This data collection used 21 μs with a corresponding divisor value of 4. The sample rate then determines the maximum depth of reach of the system at this selected setting. The depth of reach at 21 μs was 23.55 meters below the transducer face (SIMRAD, 2006).
c = Speed of sound in water (m/s)
f = frequency of sound (Hz) = 190.5 kHz
From equation (1)

= 1/190000*1488/2*4
= 0.0157 meter = 01.57 cm

That is, an ES10 digital sample is 0.0157 meter apart from each other. Thus, 1500 samples limits the effective range to 23.55 meters.

For a sound wave of frequency $f = \frac{1}{T}$, it travels within time T, at a wavelength (λ).

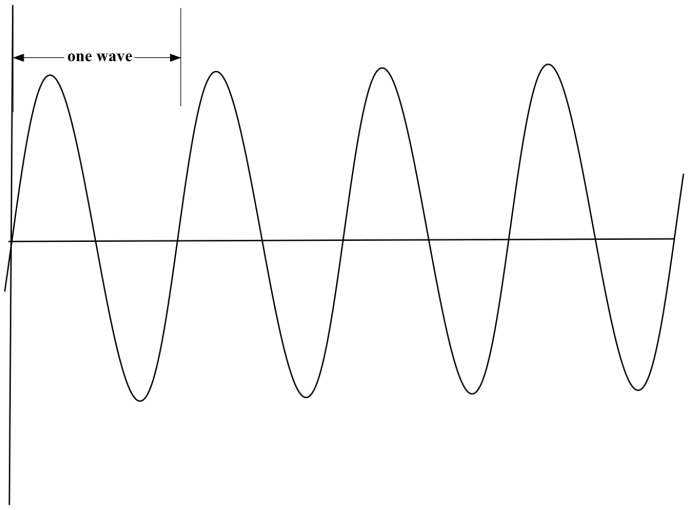

Therefore the time (T) $= \frac{1}{F}$

T = 1/190500

T = 5.26 X 10^{-6} sec

The wavelength of this wave (λ) = sound speed (c) / frequency (f)

Wavelength (λ) = 1488 / 190500

λ = 7.8 x 10^{-3} meter

For a sound wave of 190500 cycles per second at a speed of 1488 meters per second, it travels 7.8 x 10^{-3} meter in one wave. This wave travels 190 cycles per 1 ms. The pulse duration is 0.33 millisecond (ms); therefore this sound travels 190.5* 0.33 = 57 cycles over one pulse.

From the ES10 echo sounder system, the sample rate is 21x10^{-6} sec. The samples are collected every 21x10^{-6} sec within the entire length of the echo.

When sound waves travel from the transducer to a target and returns, the distance between the transducer and the target is measured by combining the speed of sound as well as the time of flight (a 2-way travel to and from the target, thus T/2). For two targets to be distinguished from another in time domain, the targets must be half pulse length apart. This is due to the two-way time of travel to and time of return from the target. The target resolution = speed of sound x pulse duration /2 = c*τ/2.

The pulse duration is 0.33 ms

Therefore the target resolution is = 1488*0.33/(2*1000)

= 0.246 meter apart.

The target resolution is the minimum distance the two single targets must be apart before single target detection can be carried out efficiently. Therefore targets less than 24.6 cm from each other cannot be sorted into single targets.

Within the ES10 system, the sample interval = 0.0157 meter,

The total number of samples that constitute a resolution = target resolution/ sample interval = 0.246/ 0.0157 = 15.6 samples

Targets are expected to be about 15 samples apart for effective single target resolution. These 15 samples constitute the pulse envelope. The echoes which are not more than $c*\tau/2$ apart are ignored, since it is impossible to distinguish between these two echoes. The envelope of the ping is the curve showing the amplitude.

When a pulse is sent through the water and reflected echo received from a target, at the pulse duration of 0.33 ms, the target amplitude is composed of 15 samples. The curve of this echo is the envelope of the pulse.

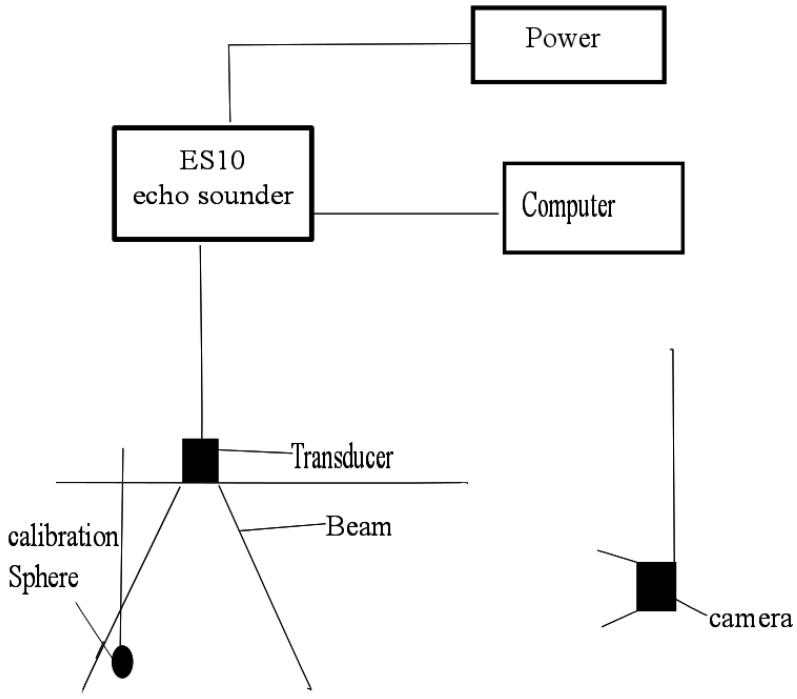

Figure 9. A schematic diagram of data collection and calibration with the ES10 echo sounder. All data were stored on PC for later analysis.

2.2.1.1 Acoustic instrumentation

The SIMRAD ES10 echo sounder (200 KHz) with the following parameter was used:

Table 1. System properties and settings of the single beam echo sounder using in data collection and calibration at Austevoll

Parameters	**Unit**
Beam Type	Single beam
Transducer type	ES10
Central Frequency	190.5 kHz
Typical Power consumption passive	0.5 W (14.0 V)
Pulse duration	0.33 ms
Sample interval (μs)	21
Number of samples per ping	1500
Half power beam angle	28^0

2.2.1.2 Single beam echo sounder calibration

The calibration was carried out using the standard reference target method (Foote et al., 1987) on 05th December 2014 at 11:45am, at the Austevoll Aquaculture research station (IMR). For the calibration of the ES10 single beam echo sounder, a standard tungsten carbide sphere of 38.1 mm diameter (TS of -39.2 (dB), 6% cobalt binder, spec size ±25 μm) sphere manufactured by Spheric-Trafalgar Ltd was used. The sphere was suspended below the transducer using a fishing rod equipped with manual reels with monofilament nylon line. The sphere was moved in the plane perpendicular to the acoustic axis in order to find the maximum sphere echo, i.e. centre of acoustic beam. Oceanographic information was collected using a CTD (STD/CTD-model SD204, manufactured by SAIV A/S, Norway).

Figure 10. A picture showing the CTD with ropes being attached.

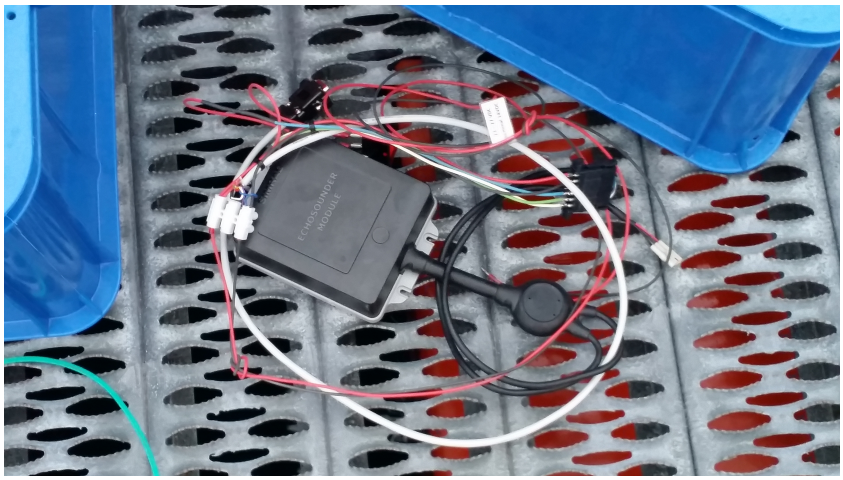

Figure 11. A picture showing the single beam echo sounder (ES10-200TCD).

From the CTD profile the speed of sound in water was calculated using Leroy 1969 proposed formula from (Simmonds and MacLennan, 2005).

The speed of sound in water was calculated as

$$\text{Speed of sound (c)} = 1492.9 + 3(T - 10) - 0.006(T - 10)^2 - 0.04(T - 18)^2 + 1.2(S - 35) - 0.01(T - 18)(S - 35) + \left(\frac{D}{61}\right) \quad (2)$$

Where T = Temperature (^{o}C)

S = Salinity (psu)

D = Depth (meters)

C = Speed of sound in water (m/s)

This formula is valid to 0.1 m/s for temperatures from −2 to 23 °C, salinities from 30 to 40 psu and depths less than 500 meters.

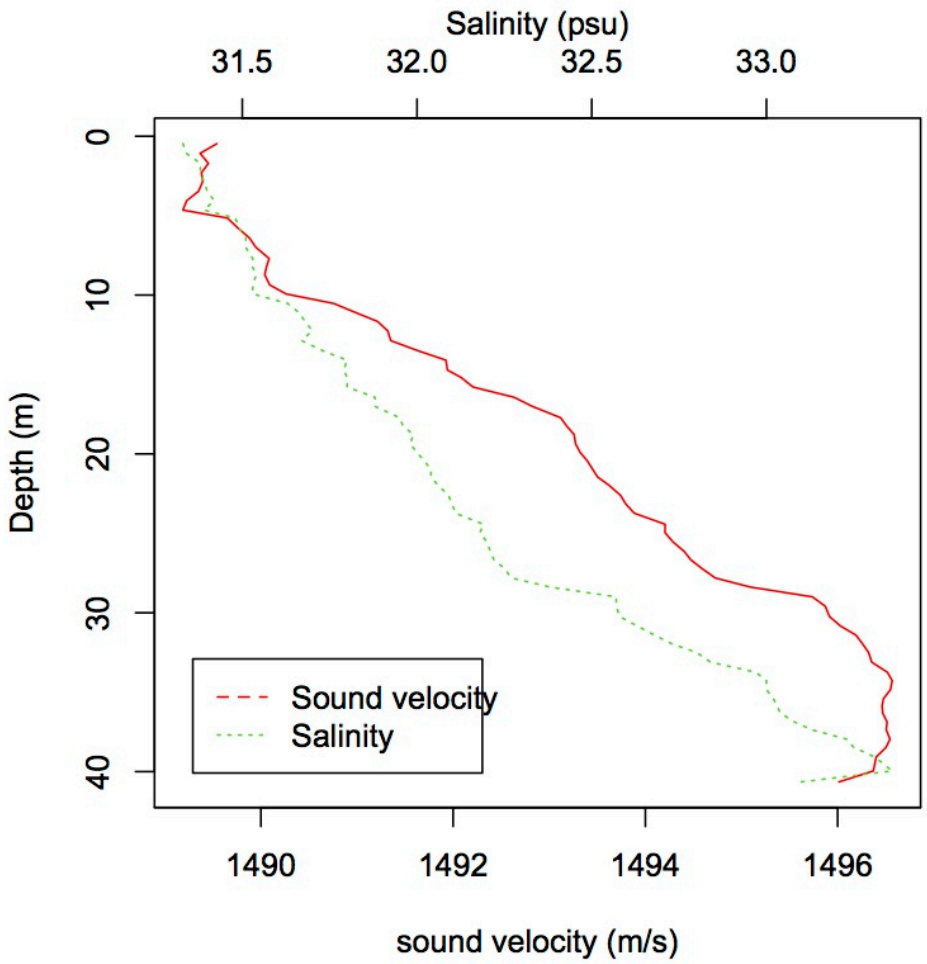

Figure 12. Plots of the CTD profile showing salinity and speed of sound in water. The values of speed of sound at 5 meters were used for the data analysis.

The calibration process

The echo sounder is calibrated to correct the data for deviations in amplitude from a nominal manufacturer setting. The difference between the expected backscatter of the sphere and the measured backscatter of the sphere is the transducer gain.

From the sonar equation,

$$I_r = I_o * \sigma * \frac{10^{-\frac{2\alpha r}{10}}}{r^4} * b^2(\theta,\phi) \qquad (3)$$

The I_r and I_o are the received and transmitted intensities respectively.

The sphere was moved continuously through the beam to ensure that sphere was observed throughout the beam. Therefore, $b^2(\theta,\phi)$ the beam directivity effect which are not accounted for in a single beam system, and can only be removed if the target is moved to its maximum amplitude, where we are at the acoustic axis, and thereby $b^2(\theta,\phi) = 1$

With range compensation factor of 40*log r TVG which was also added to account for the range independence of the target, thus $\frac{10^{\frac{-2\alpha r}{10}}}{r^4}$ is also accounted for. The gain of the transducer is g_o

Therefore the sonar equation of the calibration of the system with a known target at acoustic axis is:

$I_r = I_o * \sigma * g_o$

The echo of the sphere

$$\sigma = \frac{I_r}{I_o * g_o} \qquad (4)$$

If the expected echo of the sphere and the measured echo of the sphere are not equal

$$\sigma_{ex} \neq \sigma_{sp}$$

$$g_o \neq 1$$

Therefore $\Delta\sigma = g_o$

$$g_o = \frac{\sigma_{ex}}{\sigma_{sp}} \qquad (5)$$

g_o is the gain of the transducer,

σ_{sp}. is the backscatter of the sphere measured with the transducer

σ_{ex} is the expected backscatter of the sphere

The σ_{ex} of the sphere used is -39.2 dB = 10^(-39.2/10) = 0.0001202264. Using a calibration factor, which is the transducer gain, g_o of 1, σ_{sp} was found as the maximum backscatter of the sphere.

$$\sigma_{sp} = \frac{\sigma_{ex}}{g_o}$$

$$\sigma_{sp} = \frac{0.0001202264}{1}$$

$$= 33569.8 = 10 * \log10\ (33569.8) = 45\text{dB}$$

Therefore, the calibration factor used for data analysis;

$$g_o = \frac{\sigma ex}{\sigma sp}$$

$$g_o = \frac{0.0001202264}{33569.8}$$

$$= 3.58e-09 = 10 * \log10(3.58e-09) = -84.46\ \text{dB}$$

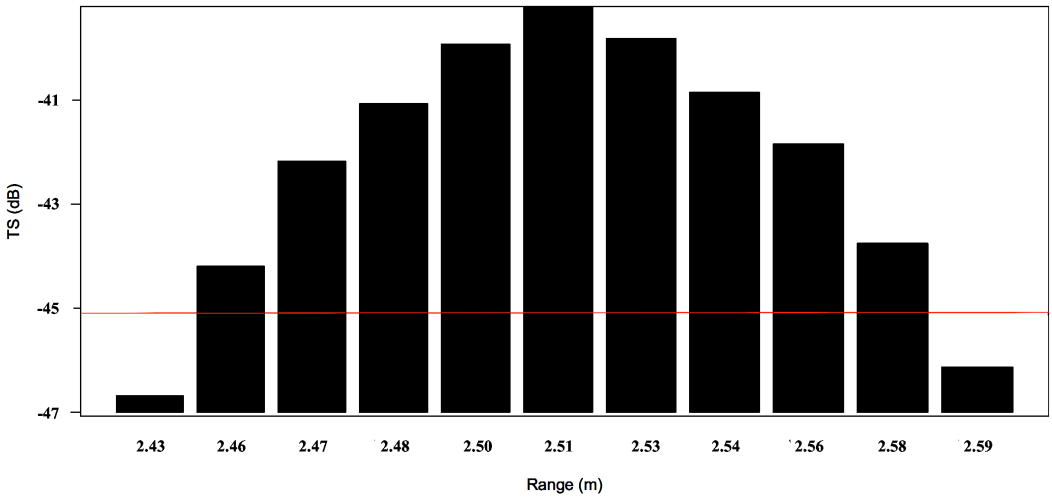

Figure 13. A figure showing the TS (dB) and range (m) of the sphere echo.

The target strength of the sphere and the -6 dB level below the peak, where the effective pulse length can be measured, indicated as vertical line (red line) in the graph. The gain of the system is simply the difference between the measured echo of the TS of the sphere and the theoretical TS of the sphere.

2.2.1.3 Data collection procedure

The transducer was attached to a rod and lowered into an empty cage space at the facility close to the open sea. The transducer was attached firmly to the cage pointing vertically downwards into the water to ensure reduced movement of the transducer. The transducer was also connected to the echo sounder. The echo sounder was connected to a power source at 14 V, 0.5 W and to a computer running a dedicated programme Labview. The Labview programme is used for capturing and logging of all the data from the echo sounder. Echo sounder data logging was carried out throughout the entire trip from 4th December through to the morning of 6th December 2014. The data were saved as *"txt"* files along with a parameter file of same name. A video capturing programme, Camtasia studio was installed to continuously record the screen display of the echogram by the ES10 platform.

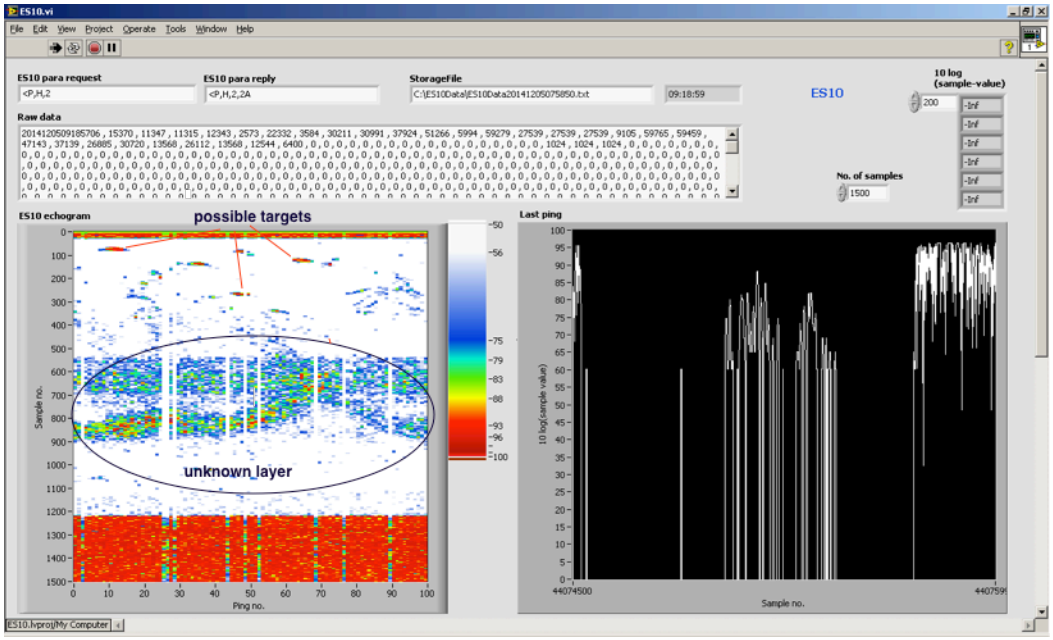

Figure 14. A screen shot of the echogram from the Labview programme during data collection.

An underwater HERO 3, manufactured by GOPRO, was also attached to a 5-meter rod and placed at a distance away from the transducer in order not for the camera to fall within the transducer beam. The camera was pointed in the direction of the transducer to record the fish species schooling within the area and coming in and out of transducer beam (See **figure 15** below showing a shot from the camera). This was only done

during the day and also close to the surface of the water where most of the targets were found swimming. Visibility at night was too low for image analysis. See **figure 16** below. It shows the data collection process.

Figure 15. A picture showing a target recorded with the camera. The target identified as saithe.

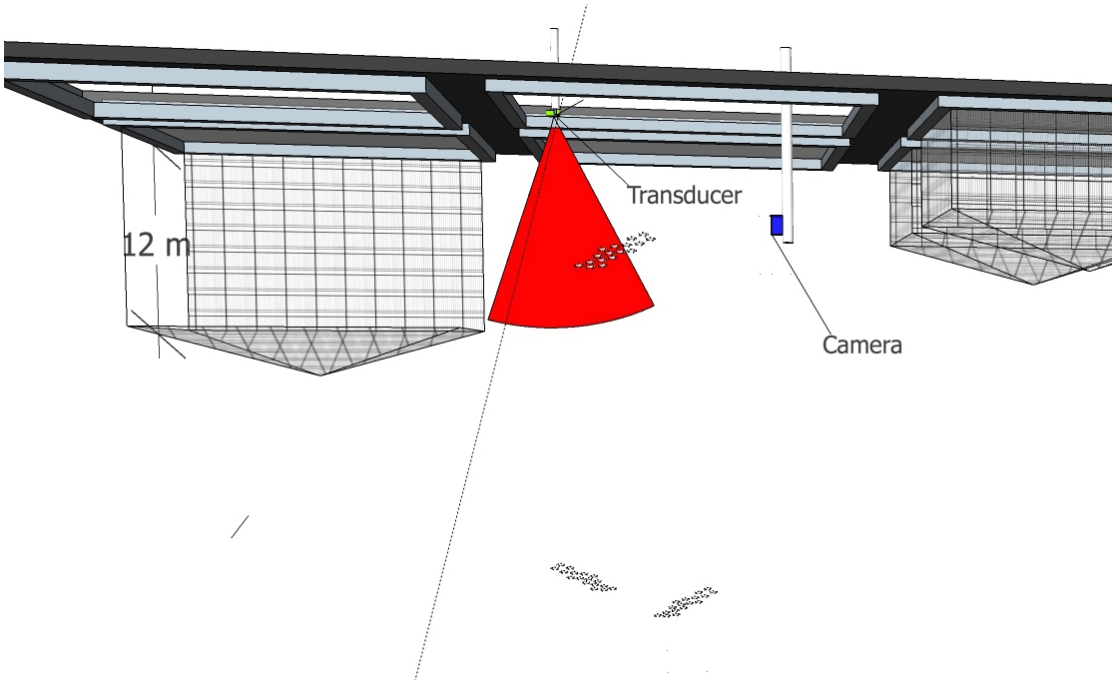

Figure 16. A diagram showing the camera and the transducer position within the study area.

2.2.2 Split beam data

The split beam data that was used in this study was collected on a scientific survey. The data was collected and stored as "raw files" on Norwegian Research vessel "G. O. Sars" by the Institute of Marine Research, Bergen.

2.2.2.1 Acoustic instrumentation

Table 2. System and parameter settings for split beam echo sounder for data collection.

Parameters	
Vessel	"G. O. Sars" (Norway)
Echo sounder	SIMRAD EK60
Beam Type	Split beam
Transducer type	ES-38-7CD
Frequency	38 kHz
Gain	26.6 dB
Transmit power	2000 W
Pulse duration	1024 ms
Sound velocity	1470 m/s
Half power beam angle	-21^0

2.2.2.2 Calibration

The calibration was carried out using the standard target reference method recommended by Foote et al. (1987). This is same way as in the single beam echo sounder prior to the survey. Unlike the single beam, the position of the sphere is also measured by the split beam echo sounder.

2.3 Theoretical approach

The target strength (TS) of a fish is a logarithmic expression of backscattering cross-section (σ). Backscattering cross section is the amount of incident energy that backscatters from the target. The backscattering cross-section is expressed in units of area square meters (Simmonds and MacLennan, 2005). When a sound signal is sent from an active echo sounder, at a target range (r), the sound intensity spreads through the water before hitting the target. The target reflects some of the sound back to the transducer. The intensity of sound received is equal to the product of sound intensity sent through the water, the acoustic target reflection coefficient, the sound lost through absorption, the distance to the target and the position of the target within the beam.
This is expressed mathematically as:

$$I_r = I_o * \sigma * \frac{10^{-\frac{2\alpha r}{10}}}{r^4} * b^2(\theta, \phi) \quad (6)$$

This is the Sonar equation for single target
I_r and I_o are the intensities of the received and transmitted sound respectively which is measured in W/m^2. The 'α' is the absorption coefficient measured in dB/km. It is a measure of how much sound intensity is lost by sound absorption. The sound energy is normally lost through, geometrical spreading of the sound and attenuation of the sound energy. The absorption is quite frequency dependent.
The $\frac{10^{-\frac{2\alpha r}{10}}}{r^4}$ is a factor for a two-way transmission loss of the signal through attenuation and spherical spreading of the sound from transducer to target and reverse.
Also, $b^2(\theta,\phi)$ is the beam pattern factor for a signal in direction θ and ϕ.

$$b^2(\theta, \phi) = \frac{I(\theta.\phi)}{I(\theta = 0, \phi = 0)}. \quad (7)$$

The sound intensity is lower outside the acoustic axis during both transmission and reception of the sound. At the acoustic axis, $b^2(\theta, \phi)$ is 1 and gradually decreases with increasing offset angle. The 'σ' is the acoustic reflectivity of a target. It is the target ability to reflect sound, due to the sound speed contrast between the target and the surrounding water.
If the equation is converted to logarithmic measures in decibel (dB);

$$EL=TS+SL+2TL+2B((\theta,\phi) \quad (8)$$

$TS = EL-2TL-SL -2B (\theta,\phi)$

Where

EL: echo level [dBre 1μPa]

TS: Target strength [dB]

SL: Source level [dBre 1μPa at 1m]

A range dependent gain factor (g_o) called time varied gain (TVG), which allows the echo from the echo sounder to display a target any distance from the transducer within the beam with same intensity regardless of the range. When g(r) is introduced, the sonar equation for single target becomes

$g_o = 10^{-2_{\alpha}r}/r^{-4}$

$I_r = I_t*\sigma* g_o *b^2 (\theta,\phi)$

Solving for σ

$$\text{Backscattering cross-section } (\sigma) = \frac{I_r}{I_t.g_o.b^2(\theta,\phi)} \quad (9)$$

The position of the target within the beam $b^2(\theta,\phi)$ is unknown in a single beam, but it is known, and therefore carried out automatically in a calibrated split beam echo sounder.

2.3.1 Backscattering cross-section (σ) and average target strength (<TS>)

The backscattering cross section is defined as

$$\sigma = 4\pi 10^{\frac{TS}{10}} \quad (10)$$

σ is the acoustic backscattering cross section (m^2)

TS is the target strength. It is the logarithmic form of the backscattering cross-section target in decibels (dB). Averaging of TS is always performed in the linear domain from averaging of backscattering cross section <σ>.

$$< \mathrm{TS} >= 10 * \log 10 \frac{< \sigma >}{4\pi} \tag{11}$$

2.3.2 Target strength and gain compensation, EK60 realisation

The target strength correction for the gain is realized in the relation

$$\mathrm{P_r} = \mathrm{P_t}.\,\mathrm{G}.\left(\frac{10^{-2\alpha r}}{4\pi r^2}\right)^2 .\,\sigma_b.\left(\frac{\lambda^2}{4\pi}.\,\mathrm{G}\right) \tag{12}$$

Where

Pr received power (dBre 1W), Pt = transmitted Power,

α = Absorption coefficient (dB/m), G = transducer peak gain = ($10^{G1/10}$),

λ = wavelength (m), σ_b = backscattering cross-section (m^2),

r = range of the target (m)

The term within the first bracket is the two-way transmission loss and the second bracket is the effective receiving area of the transducer.

The transducer gain G, is the gain located at angles θ and ϕ on the transducer surface. The one-way beam pattern of the transducer is b (θ, ϕ), and G_p is the transducer peak gain. The transducer gain (G) at angles θ, ϕ is the product of the peak transducer gain, and the beam pattern of the transducer at the two angles θ and ϕ.

That is, G (θ, ϕ) = G_p * b (θ, ϕ).

Therefore, the backscattering cross section is calculated as

$$\sigma_b = \frac{64\pi^3}{\lambda^2}.\,\mathrm{P_r}.\frac{1}{\mathrm{P_t}.\,\mathrm{G_p^2}} .\frac{1}{b^2(\theta,\phi)} .\,(r^4.\,10^{2\alpha r}) \tag{13}$$

Converting into TS,

$\mathrm{TS} = 10\log 10\sigma_b$

2.3.3 Beam pattern compensation

In the split beam echo sounder, the exact position of the target within the beam is known. The beam pattern compensation is realized by moving the points into the acoustic axis where both athwartship and alongship angles are zero. Thus $b^2(\theta,\phi) = 1$

This is by the formula

$TS_{comp} = TS_{uncomp} + 2B(\alpha, \beta)$

Where $TS_{comp,}$ is target strength compensated, TS_{uncomp} is target strength uncompensated at positions α and β and where B (α, β) is the beam compensation function.

The one-way compensation is approximated by the polynomial function

$$B(\alpha,\beta) = 3\left[\left(\frac{\alpha-\alpha 0}{\frac{\Phi\alpha}{2}}\right)^2 + \left(\frac{\beta-\beta 0}{\frac{\Phi\beta}{2}}\right)^2 - 0.18\left(\frac{\alpha-\alpha 0}{\frac{\Phi\alpha}{2}}\right)^2 . \left(\frac{\beta-\beta 0}{\frac{\Phi\beta}{2}}\right)^2\right] \quad (14)$$

Where

Φ_α is the half power beamwidth of the transducer in the alongship angle (α)

Φ_β is the half power beamwidth of the athwartship angle (β)

The beam width of -3 dB is used.

This compensation is carried out in the EK60 automatically. In the calibration, this was done using data from the measurements of the calibration sphere in many positions across the beam. The single beam ES10 echo sounder however is not capable of carrying out the beam pattern compensation, thus targets within the beam are assumed to be a random distribution.

2.4 Data Processing

The "R" statistical software package was used to create algorithm based on the single target recognition by Ona and Barange (1999). (**Appendix D** [Data analysis in the R software] and **Appendix B** [For the criteria for single target detection])

2.4.1 Single beam data analysis procedure

The ES10 echo sounder delivers 1500 TVG (20log r+ 2αr) compensated data samples for every ping irrespective of the depth of the target. A 20*log r TVG was added to the data for TS analysis.

Converting samples into Range

Range of samples (r) = S* SIr

Where S is the sample number, SIr is range sample interval

From the equation of the raw data sample interval in water,

At a sample rate of 21 μs, Range sample interval = 0.01575 meter/sample

From the sonar equation

$I_r = I_o * 10^{-2_{\alpha}r}/r^4 * b^2(\theta)$

$$EL = SL+TS - (40\log R+2\alpha r)+2B(\theta) \quad (15)$$

$TS = EL - SL+TVG - 2B(\theta)$

$TS = EL - SL + 2B(\theta)$

The location of the target within the beam in a single beam echo sounder is unknown. The TS in ES10 is equivalent to TSU, uncompensated TS in EK60.

Extracting a calibration factor for the sphere

The "txt" data for the calibration was imported and read as a function in R. Included in the function is the central frequency, average speed of sound of 1488 m/s, absorption coefficient, time varied gain, and a calibration factor of one. The data was read as a matrix with a theoretical calibration factor of one and was later displayed graphically to show the sphere within the beam (See **figure 17** below showing an echogram). The TS was extracted from between 1 and 5 meters where the sphere was located within the beam and the maximum TS taken as the TS of the calibration sphere. The ratio of the measured TS of the sphere to the theoretical TS of the sphere is the calibration factor of the echo sounder as backscatter (**APPENDIX D**).

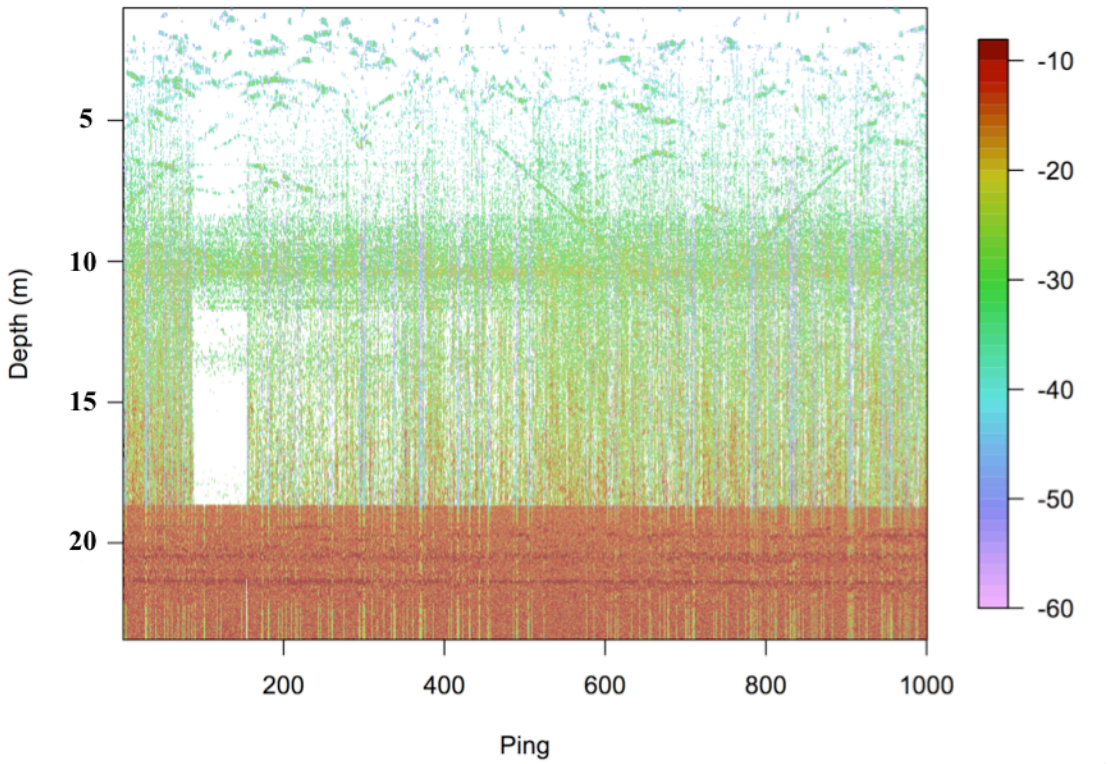

Figure 17. An echogram from the single beam data showing 1000 pings

Obtaining the target strength from the acoustic data

The calibration factor was put into the sonar equation function and the data was imported and displayed. The video recordings from the Camtasia programme of the data displayed in the Labview platform (See **figure 14**) indicated that the fish were between 1 and 5 meters away from the transducer. The data was thus truncated to within this limit for further analysis.

2.4.2 Split beam data analysis procedure

A function was created to read EK60 "raw" file. Using the libraries "fields" and "R.utils", the file was sourced from a directory and the data was read. The frequency, sample interval, pulse length, average speed of sound, absorption coefficient and length of beam are the main parameters extracted for further analysis.

A list was created to contain the main parameters thus allowing the script to access them. A time varied gain (TVG) was added thus making the acoustic reflectivity of the

target irrespective of the range of the target. A 2D echogram of the data is displayed regulating the depth, number and range of pings needed and the colour scale to allow easy visualisation (See **figure 18** showing the echogram of the split beam data).

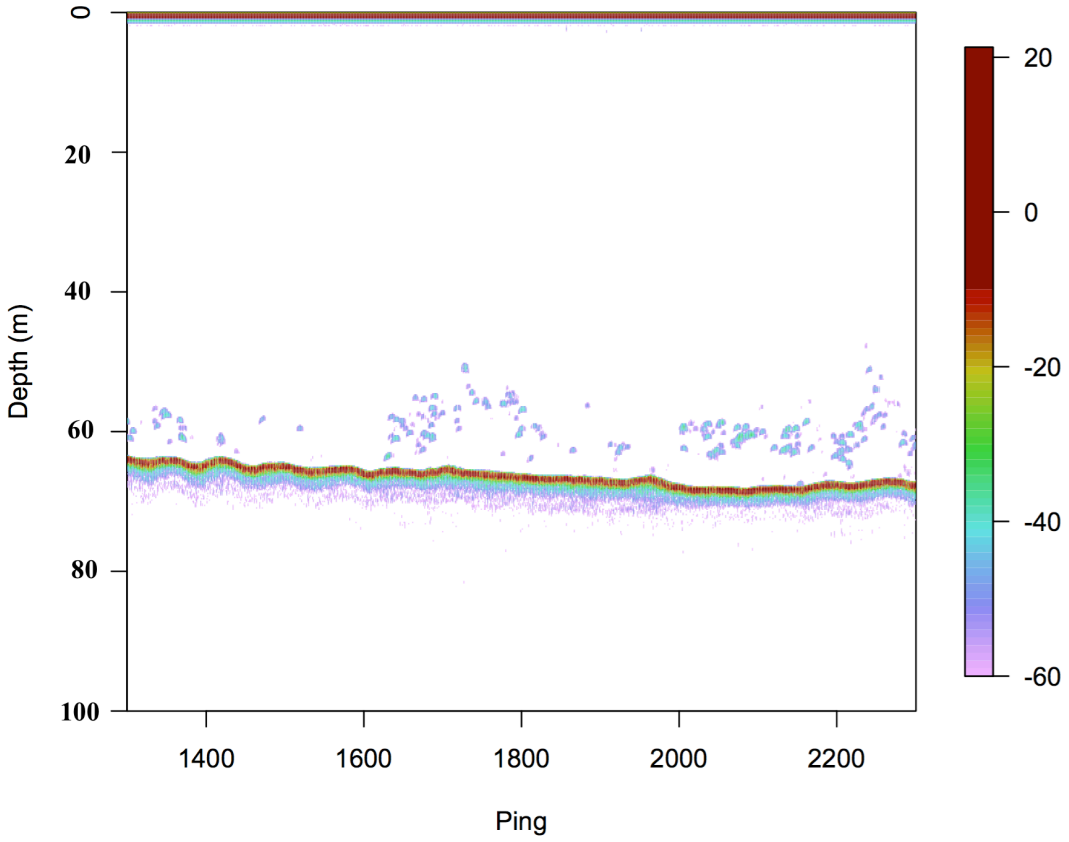

Figure 18. An echogram showing 1000 pings from the split beam data.

2.4.3 Single echo detection (SED)

The single echo detection is often used interchangeably with the single target detection. The entire data analysis was carried out on a ping-by-ping basis. Through the visualization of the echogram, a single ping with known target was selected. Single target detection analysis was carried out on this ping with known target and reiterated to detect single targets on every ping.

Filtering single ping data

A noise echo is an echo too low or too high to be originating from a single fish. A threshold was set to remove noise, transducer near field and bottom echo. The noise threshold was set at TS greater than -60 dB or less than -10 dB. These echoes are either too high or too low to have originated from a single target fish with a swimbladder. The near field of the transducer is the zone where the actual acoustic beam is not entirely formed, and the sonar equation is not valid here. Taken the linear dimension of the transducer surface as X,

$$\text{Near field (Rn)} = X^2 / \text{wavelength } (\lambda) \qquad (16)$$

For the 38KHz transducer, the near field corresponds to
$(0.3)^2 / 0.039 = 2.31$ meters

For the ES10 transducer;
Near field (Rn) = $(0.05)^2 / 0.0078 = 32.1$ cm.

The bottom removal in the ES10 dataset was not carried out in the single beam analysis because the data was truncated at 5 meters below the transducer surface. The bottom was at 23 meters and therefore the bottom was automatically removed (see **figure 19** showing the position of possible targets within a ping and the target strength). In the split beam echo sounder however, bottom removal was carried out using a series of algorithm. The bottom TS was greater than -20 dB, thus the bottom candidate was taken as an acoustic sample beyond which TS is greater or equal to -20 dB, and 10 samples about this sample. This sample is taken as the first bottom candidate. In the next ping, the bottom candidate is 5 samples below the minimum bottom candidate and 5 samples above the maximum bottom candidate with TS greater or equal to -20 dB. This is reiterated to give the bottom.
A histogram of the TS of the ping with bottom, noise and near field removed was displayed as a plot. The median of the TS was retrieved and a threshold set at -55 dB less than the median TS. This histogram allows visualizing the distribution of the target strength of the beam.

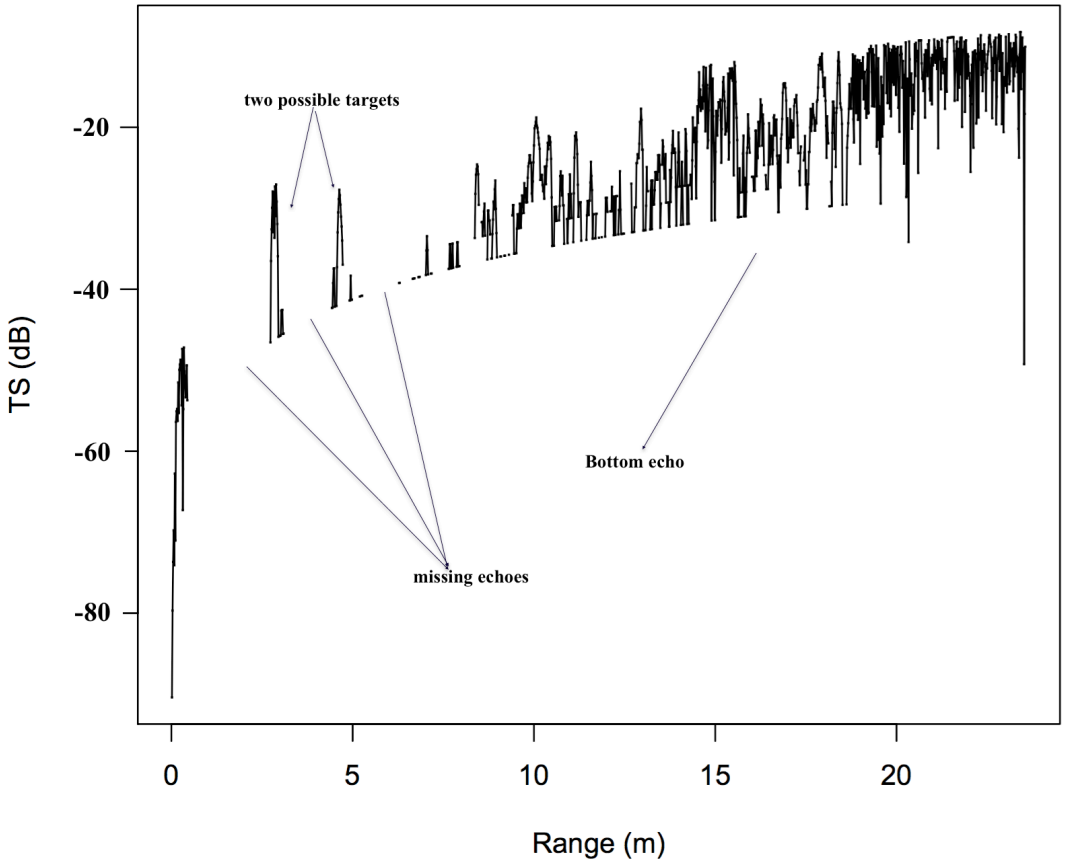

Figure 19. A single ping display of echo along the entire range of the samples from surface of transducer to depth and the TS of the samples

Table 3. Parameters settings: single target detection.

Parameter	Value
Maximum TS threshold	-20 dB
Minimum TS threshold	-55 dB
Maximum echo length	1.5
Minimum echo length	0.5

TS threshold

The TS window set highest possibility of an echo originating from a target at the centre of the beam. The targets being studied have the highest possible echo at -25 dB, thus the maximum echo is set to -20 dB. It is strongly recommended that threshold set to within 25 to 30 dB from the strongest echo to the weakest echo. The minimum TS window is set at -55 dB.

The pulse duration window

This threshold is set at -6 dB relative to the peak amplitude. Echoes from singe targets are expected to be within the maximum echo length and the minimum echo length window.

To find the effective pulse length of the single target, the area under a plot of TS versus range of the identified echo was calculated. The area was calculated from the peak echo to -6 dB below the peak.

From the ping studied,

Area = total sum of the product of intensity and width at every point

Area under the curve at -6 dB relative to the peak, the area = -6.58 (area units)

Tau (eff) = Area/max intensity.

= -6.582 / -6

= 1.10 meters

Therefore the pulse duration window used for the analysis of single echo detection was 0.5 to 1.5. This is a range around the effective pulse duration, also allowing for pulse stretching by a large target.

Also echoes that are too close in vertical range at the -6 dB threshold are rejected since this could be originating from overlapping echoes.

This is carried out in the script as follows;

A function that extracts target strength was created to extract TS from the filtered single ping. Single target detection conditions are set to accept or reject detection in a ping as a single target. An echo from a target is accepted as a single target if that echo is valid for all the single target criteria

Step 1:

A TS threshold was set defining the limit of TS within which a single target of the fish may occur. The maximum TS was set at -55 dB and the minimum TS at -20 dB. The ping was valid only if the TS was within this Threshold.

Step 2:

An echo from a ping is accepted if the pulse length of the ping is valid. A valid pulse length is defined as (pulse length / sample interval)*sample range. A valid echo length is 0.5 to 1.5. Single target candidates were valid if the length of TS of the target is valid else it is false, and thus defined as NA´s.

Step 3:

For an echo from a multiple target that was not detected by TS threshold filter, an unbroken sequence of length of the echo was defined and the effective length of the candidates retrieved. A -6 dB TS relative to the peak was applied and the accepted candidates selected. When the pulse length and effective beam width are valid for that target, this is selected as a single target. Therefore, the mean backscatter of a single target in a particular ping was collected as backscatter of a single target. The TS of single echo detections were displayed for all the pings. A histogram of single detections was plotted showing the mean backscatter expressed as TS, the total number of detections and the standard deviation of single detections. The single detections were further analysed to form tracks.

2.4.4 Target tracking

Target tracking isolates TS detections originating from single targets combined into a single track. It is a ping-by-ping analysis of the target movement through the insonified water volume. This is important since it reduces ping by ping variance which could complicate *in situ* estimate of fish size from target strength (Ehrenberg and Torkelson, 1996).

Table 4. Parameter settings: single target tracking.

Parameter	Split beam	Single beam
Minimum TS [dB]	-55	-55
Max. Sample difference in range between pings	-	3
Minimum track length [number of detections]	10	10
Maximum number of subsequent missing pings	2	3

The first ping (n_i) with single detection and the subsequent valid ping (n_i +1) with a single detection must be within a set number of pings from each other. That is, (n_i +1) - (n_i) < = 2 pings for split beam and (n_i +1) - (n_i) < = 10 pings for single beam.

For step two, the track is valid if the TS detection in the ping n_i +1 is within ± 3 samples from ping n_i.

For step 3 a track is valid if the total number of successive detections in the same range are more than 10. That is, number of detections in n and n+1 ≥ 10.

A track is accepted if it satisfies all the criteria for target tracking.

The valid tracks for single fish were extracted and a histogram is plotted showing the mean backscatter of the track, the number of tracks, the standard deviation for the same data for which the untracked detections were carried out on. The results between the tracked and untracked data are compared.

2.4.5 TS – fish length relationship

The TS - length of fish relation has been established for certain species with precision in experiment. It is however often more difficult for swimbladder bearing fish than for non-swimbladder bearing fish (Bertrand et al., 1997). The TS is related to the length of fish by the relation, TS = a log10 (L) - b where ‘a’ and ‘b’ are constants and are specific to the specie and the frequency used. Bertrand and Josse (2000) investigated TS – fish length at 38kHz and found that;

Yellowfin tuna: TS = 25.26 log10 (FL) - 80.62;

Bigeye tuna: TS = 24.29 log10 (FL) - 73.31.

Nakken and Olsen (1977), carried out an ex-situ measurements on saithe and the resultant equations were $\overline{\mathrm{TS}} = 23.3\log_{10}(\mathrm{L}) - 64.9$ at 38khz and $\overline{\mathrm{TS}} = 20.1\log_{10}(\mathrm{L}) - 60.1$ at 120 kHz. It is however argued that during in-situ measurements, 'a' is consistently close to 20 and thus assumed not to be significantly different from 20 (Simmonds and MacLennan, 2005).

Thus, TS = 20 log10 (L) - b20 value.

From Nakken and Olsen (1977), TS of Saithe at 38 kHz offsets from TS at 120 kHz by 4.8 dB higher. This value is similar to Pedersen and Korneliussen (2009) who found the mean TS at 38 kHz to be 4 dB higher than mean TS at 120 kHz and also 6 dB higher than mean TS at 200 kHz.

The TS – length equation used in the script for the target strength – fork length analysis was

$$\overline{\mathrm{TS}} = 20\log_{10}(\mathrm{L}) - 68 \qquad (17)$$

This equation is similar to the recommended equation for physoclists $\overline{TS} = 20\,log10\,(L) - 67.4$ (Simmonds and MacLennan, 2005).

Using the TS – length equation, the length of the fish may be calculated. A plot of the relationship between the lengths and TS is displayed **(figure 25** and **figure 26)**

2.4.6. Suggested data output for the TS of the detections

Table 5. Suggested data output.

Target	**Range of TS (dB)**
Weak	< -40
Medium	-30 to - 40
Strong	> - 25
Strong and wide	> = -25, high τ,

The data transferred from the current buoy is one ping per hour because of power demand.

CHAPTER THREE

RESULTS

3.1 Calibration

There was difficulty in visualising the sphere in the beam during the single beam calibration. The value of speed of sound from the CTD data taken during the calibration was 1488 m/s differing from the prior expected value of 1500 m/s. This value was taken from 5 meters below the surface where the detections of targets were observed within the beam on the up-cast data. The temperature had narrow range from 10.9 to 12.3 $^{\circ}$C with the salinity following almost same pattern with range from 31.3 to 33.4 psu.

3.2 Single pings analysis

The analysis of the data was carried out ping by ping. The TS distribution of a typical ping with possible target shown graphically below similar to Figures

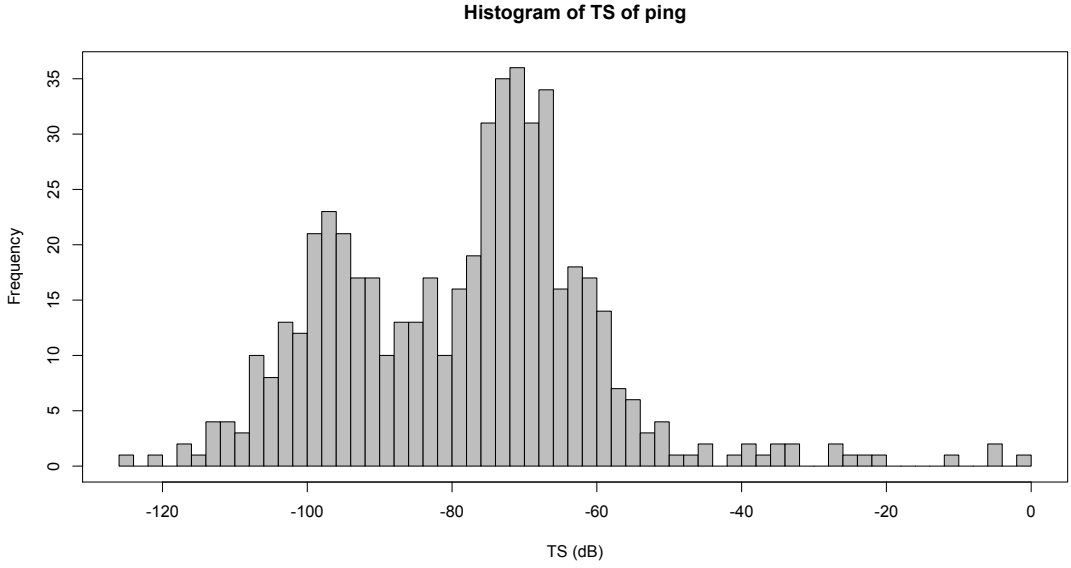

Figure 20. A figure showing the histogram of distribution of TS of a single ping.

TS less than -60 dB were regarded as noise in this system, and TS above -20 dB were the bottom echoes. The TS range between -60 dB and -20 dB were analysed for fish targets**.**

3.3 Target strength measurements

Single target strength measurements carried out for split beam and single beam raw data. The single target detections were also tracked for possible echoes from a single fish to be predicted. Target tracking lowers the variance within the estimate of target strength of each fish target (Ehrenberg and Torkelson, 1996).

3.3.1 Target strength measurements from split beam

The target strength distribution shows a bimodal distribution with the mean modal target strength (<TS>) for the data was – 34.2 dB. This could mean about two-length class of fish gathered in the area, though the modes are not very distinct. There were 5504 single echo detections over the entire 3319 pings with a standard deviation of 8.5 dB. The high value of the standard deviation could be as a result of the high variation with in the detections

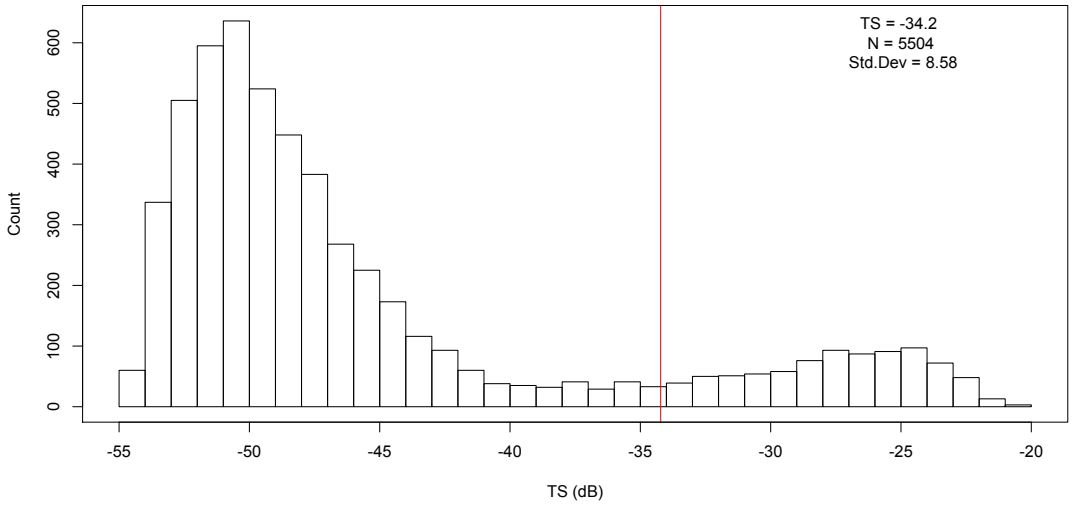

Figure 21. TS distribution of single target detections and the vertical line indicates the mean TS and standard deviation of 8.55 dB.

At 95 % confidence interval, the ranges of mean -34.44 to -33.98. The mean of -34.21 ± 0.23 dB.

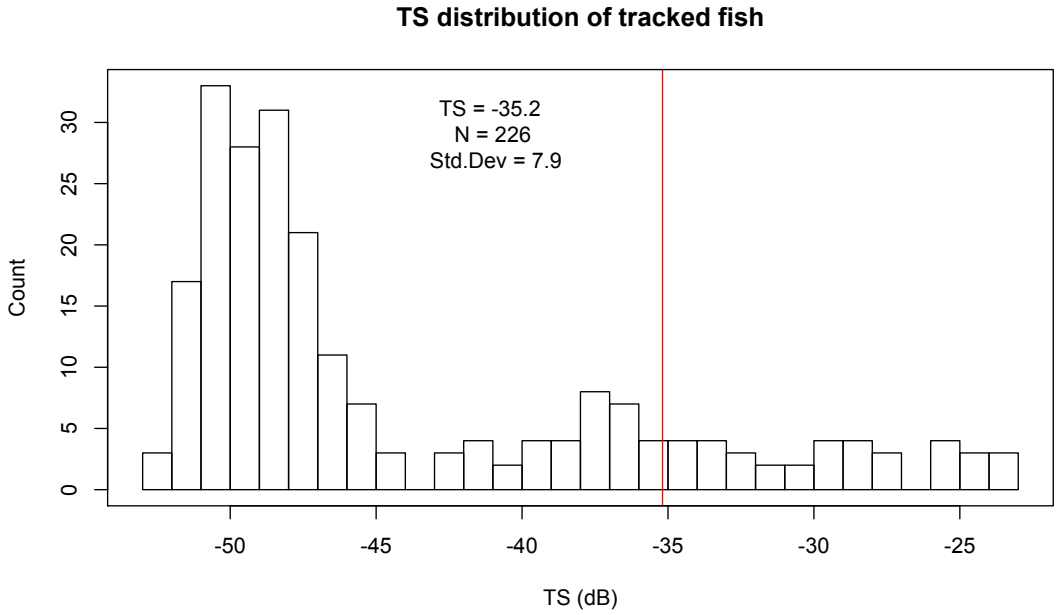

Figure 22. A plot showing the distribution of TS of tracked fish and the vertical line indicates the mean TS at -35.18 dB and a standard deviation of 7.9 dB.

At 95 % confidence interval, the ranges of mean 36.22 to -34.16 dB's. The mean TS therefore is -34.21 ± 1.03 dB. Tracking reduced the mean standard deviation within the split beam data from 8.55 dB in the untracked data 6.9 dB in the tracked data as expected.

3.3.2 Target strength measurements from single beam

The data used for the target strength measurements constituted data collected for the entire duration of data collection in Austevoll. The data files saved in different files were displayed consecutively and single target detection analysis carried out. There was a constant layer within the middle section of the beam that was attributed to the side lobes echo from the installations around the fish cages. The possible targets within the beam were found from the echogram to be within 5 meters below the surface of the transducer. This layer seen from the echogram did not affect the target strength measurements from the single beam analysis because the data analysed was selected within the range of 1meter and 5meters. This area was where detections were found within the beam.

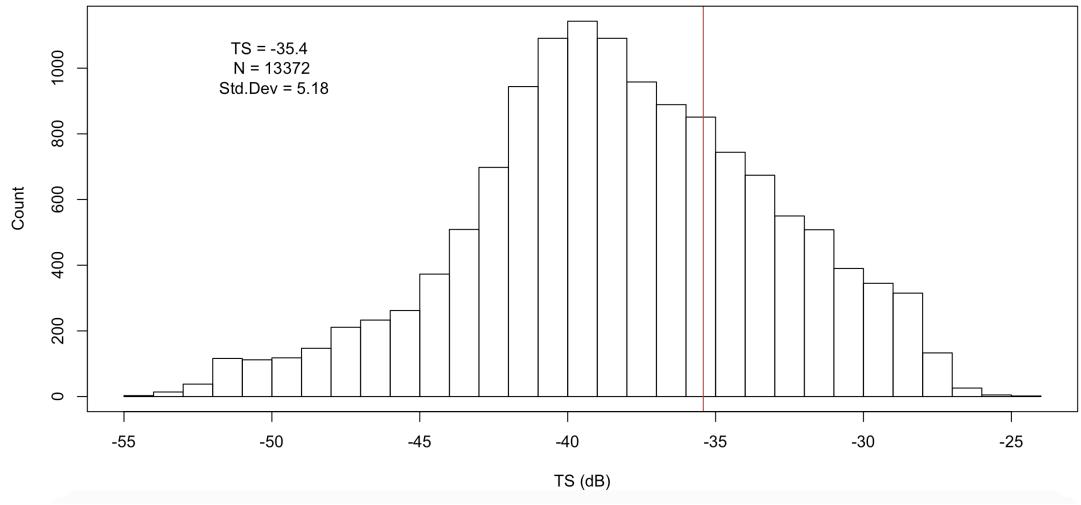

Figure 23. Target strength measurements of tracked fish detections.

The vertical line (red line) shows the mean TS at -35.42 dB and standard deviation of 5.18 dB. At 95 % confidence level, the mean TS is -35.51 to -35.33. The mean target strength at 95% confidence interval is -35.42 ± 0.09 dB.

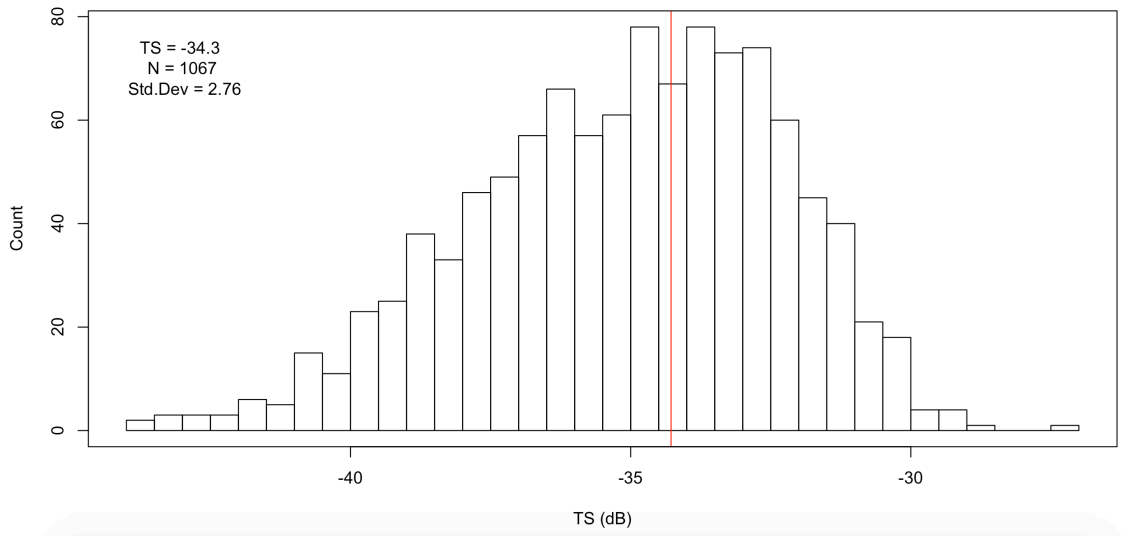

Figure 24. Target strength measurements of untracked single target detections.

The vertical line shows the mean TS at -34.3 dB and standard deviation of 2.78 dB. At 95 % confidence level, the mean TS is -34.47 to -34.13. The mean TS at 95% confidence interval is -34.32± 0.17 dB. The variance is lower than the variance of untracked detections as expected.

3.4 Target strength- fish length relationship

The Length of fish measured from the target strength using the equation suggested is displayed graphically below.

3.4.1 Split beam TS – fish length

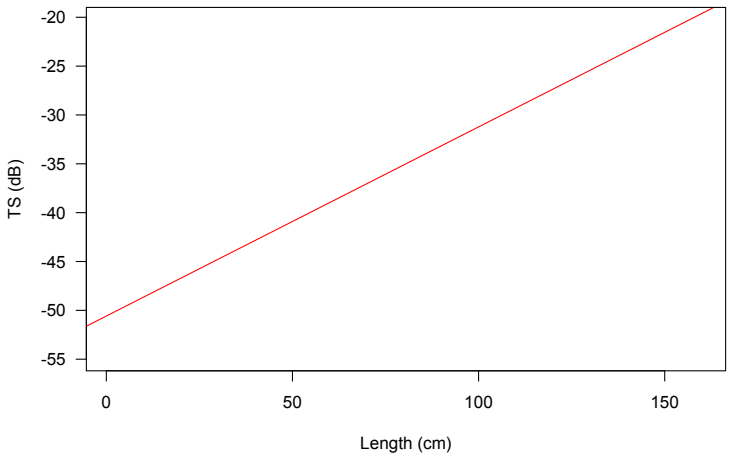

Figure 25. A plot of TS and length of fish of the split beam SED data.

3.4.2 Single beam TS – fish length

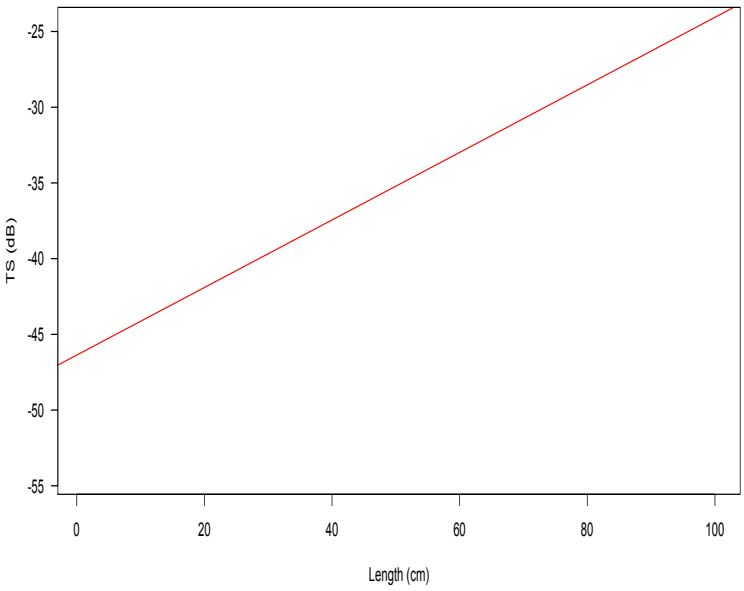

Figure 26. A plot of the TS - length for SED in the single beam. Using the equation TS = 20*log10 (L) – 68.

The measured mean target strength is about -35.42 dB from the SED, which will indicate that this fish is about 42.6 cm. The assumption used infering that target strenth – length relationsip is same for saith as for cod is only true to some degree. The ‘b’ constant may well differ from the -68 used. The maximum TS in the TS distribution may also indicate how large the fish have been, as indicated by Nakken and Olsen (1977). That the TS - length can be used to convert maximum TS to size.
In this application, using a single beam , without beam pattern compensation, the mean TS is expected to be underestimated by about 2.5 dB. This error may be corrected for in the TS distribution. The sole purpose of this workis to discriminate between very large target such as the tuna, and relatively smaller targets about 20 dB’s weaker, juvenile tuna and bait fish about 30 dB’s weaker. This correction was not carried out. Moreover, due to power demands and limitations thereof, the echo sounder can not run at full pin rate but about 1 ping per hour. This ping must therfore be analysed for strong and weak echoes, and susequently the decision on target group strength must be taken on very few pings, with no tracking possiblilities.

3.5 Realistically proposed data transfer format

The data transfer format from the FAD and Argos system must be compressed to reduce the cost of transmission. We therefore suggest that the water column is grouped into 10 layers, where the echo integral is indicated. Where the number of each of 4-echo strength categories is coded in ASCII characters, supply with an extra string.
The system to minimise this text string is not part of this thesis, but a 10 dB step and an indication of the number of detections of each category in each of the channels. The total category from 5 to 100 meters may be used if the message is too large. Moreover, the skipper’s interest is on stronger categories where high abundance is registered.

CHAPTER FOUR

DISCUSSION AND CONCLUSION

4.1 Error sources

4.1.1 Instruments

Echo sounder calibration is carried out to help provide accuracy in the target strength measurements and subsequent fish mean target strength estimates. There are many factors that affect proper calibration of the echo sounder particularly at short range (Foote et al., 1987; Ona et al., 1996). It is therefore recommended that increased range between 15 to 25 meters below the transducer surface can mitigate some of these range dependent factors (Ona et al., 1996). In the single beam echo sounder calibration, this recommendation was not adhered to because of the dense sound scattering layer within the beam at 8-meter range (See **figure 27** below). It made it difficult to identify the sphere on the echogram when suspended within the beam at that layer. Also, the standard target was not clearly visible in the beam. When the echogram was plotted, the target path appeared very faint due to the nature of the echogram display.

Determination of the accuracy of the calibration performed was difficult in a single beam but less for a split beam where the actual target position is known. Here we had to rely on whether we could find the approximate centre of the acoustic beam by watching the echo strength when pulling the sphere across the beam. Also, the relatively wide beam helps, as the sensitivity varies less close to the centre in this beam, than in a narrower beam. In earlier single beam calibrations, an accuracy of 0.1 dB is claimed under favourable conditions. This is hardly possible here, but replay of the calibrated data from the calibrations may indicate better than ± 1.0 dB, which for all practical purposes in this investigation is sufficient. Ping to ping variability between successive pings on the sphere at acoustic axis is about 2 dB

.

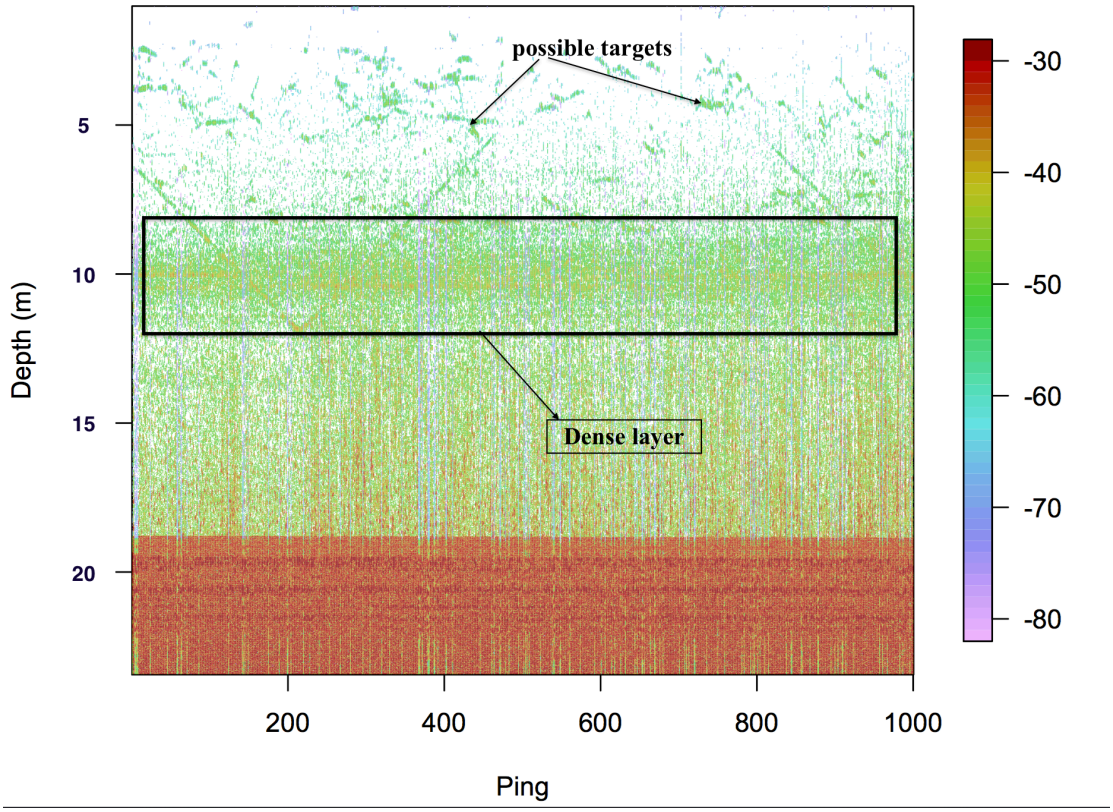

Figure 27. An echogram showing the dense scattering layer within the beam.

4.1.2 Error sources in target strength measurements and target tracking

The target strength measurements in this study had some possible sources of error. The lower target strength threshold was set at -55 dB for a single target. This was a reasonable limit owing to the size of the target. The threshold was set based on available literature from pelagic and bottom fish of various sizes (Simmonds and MacLennan, 2005) including fish less than 10cm. Moreover, the threshold may reject targets that are oriented or tilted near vertical positions. It has also been suggested that dorsally measured fish often have a target strength variation between 20 to 25 dB from the strongest echo to the weakest echo. In the single beam, the effect of the beam pattern was not critically analysed. This is because the targets were assumed to be randomly distributed within the beam. The single echo detector was largely deemed successful because the fish were loosely aggregated. Therefore very minimal error owing to multiple targets, single targets at close range could possible affect the TS measurements. The configuration of the ES10 which is equipped with a wide angle

may have low signal to noise ratio from echoes at the extremities of the beam. This possible error source however was not large enough to mask the targets. The critical parameters influencing of the equation for TS – length relationship for fish has been examined by (Boswell et al., 2008). The coefficient of the TS - fish length assumed for this work was 20, and may have errors associated with them which might be carried into the target strength estimates (Boswell et al., 2008). The arbitrary track length threshold could have affected the number of fish tracks detected. However, careful manipulations of the data using different length were carried out to ensure the most appropriate length of track was set. Different fish tracking parameters were used for both split beam and single beam echo sounder data, because the single beam recorded large number of missing pings. Thus, different criteria were needed to ensure that the tracking of fish was carried out efficiently.

4.2 Target strength measurements

Single fish echo detection can be very difficult owing to noise echoes from around the fish and missing echoes (Balk, 2001). The echoes from a target may thus be overlooked as background noise. In this study, single target detection algorithm proposed by Ona and Barange (1999) was used. Single target detections are carried out ping by ping. Therefore the number of detections does not reflect the total number of targets. Target tracking was thus carried out to segregate echoes from same target.

4.2.1 Single target detector algorithm

The single target detector algorithm ensures that echoes from single isolated targets are selected for target strength analysis. This is particularly important because it filters echoes from fish schools, noise, bottom and overlapping echoes from targets occupying similar range (Ona, 1999). The single target algorithm was carried out on calibrated and TVG compensated data. The criteria used in the algorithm are provided in the **Appendix B.** In the dispersed situations, and at short range, there is very little probability of SED failure.

4.2.2 Single fish tracking target strength measurements

Target tracking can be difficult to carry out manually in a data source with lots of surrounding noise (Balk, 2001) as appears in the ES10 data. Therefore an automatic tracking requiring the use of the ping gap between different single target detections will be a more effective way. Using the ping gap, track length and a sample number threshold between adjacent single targets, the tracking process is reiterated along the pings to produce tracks of single targets. Target strength leads to a ping-by-ping variability in the estimate of the in-situ target strength estimate. The variance in the estimated target strength can be lowered by tracking, which isolates individual fish target strength. The fish track averaged over a series of measurements of mean TS results in increased accuracy in the target strength estimates of individual fish (Zhao, 1996). It has therefore been recommended for *in situ* studies including behavioural studies (Torgersen and Kaartvedt, 2001). The tracking method can help improve our understanding of the behaviour and swimming pattern of the fish under FADs. The method used for tracking was based on the algorithm suggested by Ehrenberg and Torkelson (1996). Similar work has been carried out by using similar tools and settings (Lopez et al., 2010). The work in this thesis was specifically aimed at identifying single targets, as opposed to biomass estimate study by Lopez et al. (2010).

4.2.3. Estimation of fish length from target strength measurements

Much research has been done to establish the TS – length relationship for various fish species. Yellowfin tuna and bigeye tuna studies have also been undertaken for the TS – Length relationship (Josse et al., 1999; Bertrand and Josse, 2000). The swimbladder is affected immediately as soon as fish comes out of the water. It therefore offers a challenge for in-situ study of swimbladder bearing fish. The depth of the fish affects the shape of the swimbladder and subsequently the TS over a wide range of fish species (Lu et al., 2011). Most species of fish swimbladder grow proportionally with length of the fish. Therefore a strong correlation between the TS and the length of the fork length is expected, since about 90 % of the backscatter comes from the swimbladder (Foote, 1980).

4.2.4 Realism in the measurements relative to FAD operation

This study does not have restrictions on power supply. However, a buoy attached to a FAD has power limitations. Therefore, only a limited number of pings can be sent. It is clear that the calibration part is still valid, and all FAD echo sounders could be calibrated before delivery from the manufacturer. Real metric values and SI units of TS could then be measured with the limitations the single beam and wide opening angle offers. Target strength summary can be received, as demonstrated in this work, if the FAD is connected to a small computer sufficient for these relatively simple calculations. Several models are now available on the market that can run on solar panel, or very low power consumptions. Rasberry Pi and arduino are just a few examples. The low ping rates used (1/hr) by current buoy on FADs may be a challenge. But if the FAD collects data over days and weeks, the development of a TS distribution is realistic. Target tracking as indicated in one of my chapters is not.

4.3 Conclusion

The ES10 used for target strength measurements indicates that such simple echo sounder can be placed under FADs for fish detection. When such echo sounders are mounted under FADs for remote access, fishers do not need to travel miles to ascertain whether the FAD is productive or not. If the FAD can indicate both relative biomass in 10 layers as now, but also a indication of target size, like suggested here, it could be a helpful tool for the fishing industry. This will help reduce bycatch because fishers after travelling long miles to come to a FAD, may want to catch the fish under the FADs even when they suspect high bycatch (Lopez et al., 2010). The current echo sounders used only provide estimate of biomass for all the surrounding species and sizes of fish under FADs with no distinction (Lopez et al., 2010).

I would therefore recommend that, this system be improved through more elaborate work to provide fishers with remote data on target species and bycatch. This informs fishers on ratio of target species to bycatch species under the FADs (Lopez et al., 2010). This can also be a tool to study the behaviour of target and non-target species through tracking. And can be very effective as a measure to reduce bycatch. I am sure that more modern echo sounders, like split beam, multi-frequency and broadband will eventually

be introduced, but at this stage, the single beam systems like the one used here, are dominating the market. For FAD research however, power may not be a limiting factor. Therefore, significant information on fish community behaviour and the overall effect of the FAD in the ecosystem may be studied for months with drifting scientific equipment. In addition, a stereoscopic video camera can be involved in this study to aid species sizing and identification in such investigations.

REFERENCES

Altman, P. L., and Dittmer, D. S. 1962. Growth, including reproduction and morphological development. Growth, including reproduction and morphological development.

Amandè, M. J., Ariz, J., Chassot, E., De Molina, A. D., Gaertner, D., Murua, H., Pianet, R., et al. 2010. Bycatch of the European purse seine tuna fishery in the Atlantic Ocean for the 2003–2007 period. Aquatic Living Resources, 23: 353-362.

Aquamaps 2013a. Computer generated distribution maps for Thunnus albacares (Yellowfin tuna), with modeled year 2100 native range map based on IPCC A2 emissions scenario. . Aug. 2013 edn.

Aquamaps 2013b. Reviewed distribution maps for Katsuwonus pelamis (Skipjack tuna), with modeled year 2100 native range map based on IPCC A2 emissions scenario., Aug. 2013 edn.

Aquamaps 2013c. Reviewed distribution maps for Thunnus obesus (bigeye tuna), with modeled year 2100 native range map based on IPCC A2 emissions scenario. August,2013 edn.

Balk, H. 2001. Development of hydroacoustic methods for fish detection in shallow water. Faculty of Mathematics and Natural Science, University of Oslo.

Bannerman, P., Pallarés, P., and Kebe, P. 2005. Improvements in the Ghanaian tuna statistics collection system. Collect. Vol. Sci. Pap. ICCAT, 57: 129-136.

Bannerman, P. O., and Bard, F. X. 2001. Recent changes in exploitation patterns of tunas in the Ghanaian fishery and their effects on commercial catch at size. Collect. Vol. Sci. Pap. ICCAT, 52: 466-479.

Barkley, R. A., Neill, W. H., and Gooding, R. M. 1978. Skipjack tuna, Katsuwonus pelamis, habitat based on temperature and oxygen requirements. Fish. Bull, 76: 653-662.

Baske, A., Gibbon, J., Benn, J., and Nickson, A. 2012. Estimating the use of drifting Fish Aggregation Devices (FADs) around the globe. PEW Environment Group.

Bertrand, A., and Josse, E. 2000. Tuna target-strength related to fish length and swimbladder volume. ICES Journal of Marine Science: Journal du Conseil, 57: 1143-1146.

Bertrand, A., Josse, E., and Massé, J. 1997. Preliminary results of acoustic target strength measurements of bigeye (Thunnus obesus) and yellowfin tuna (Thunnus albacares). *In* Proceedings of the 5th Indo-Pacific Fish Conference, Noumea, pp. 443-450.

Bertrand, A., Josse, E., and Massé, J. 1999. In situ acoustic target-strength measurement of bigeye (Thunnus obesus) and yellowfin tuna (Thunnus albacares) by coupling split-beam echosounder observations and sonic tracking. ICES Journal of Marine Science: Journal du Conseil, 56: 51-60.

Beverly, S., Griffiths, D., and Lee, R. 2012. Anchored fish aggregating devices for artisanal fisheries in South and Southeast Asia: benefits and risks. FAO Regional Office for Asia and the Pacific, Bangkok, Thailand. RAP Publication, 2012/20: 65.

Boswell, K. M., Kaller, M. D., Cowan Jr, J. H., and Wilson, C. A. 2008. Evaluation of target strength–fish length equation choices for estimating estuarine fish biomass. Hydrobiologia, 610: 113-123.

Brill, R. W., Bigelow, K. A., Musyl, M. K., Fritsches, K. A., and Warran., E. J. 2005. Bigeye tuna (Thunnus obesus) behaviour and physiology and their relevance

to stock assessments and fishery biology. Collect. Vol. Sci. Pap, ICCAT, 57: 142-161.

Brill., R. W., Block, B. A., Boggs, C. H., Bigelow, K. A., Freund, E. V., and Marcinek, D. J. 1999. Horizontal movements and depth distribution of large adult yellowfin tuna (Thunnus albacares) near the Hawaiian Islands, recorded using ultrasonic telemetry: implications for the physiological ecology of pelagic fishes. Marine Biology, 133: 395-408.

Brill., R. W., and Holland, K. N. 1990. Horizontal and vertical movements of yellowfin tuna associated with fish aggregation devices. Fish. Bull, 83: 493-507.

Bromhead, D., Foster, J., Attard, R., Findlay, J., and Kalish, J. 2003. A review of the impact of fish aggregating devices (FADs) on tuna fisheries. Final report to the Fisheries Resources Research Fund. Bureau of Rural Sciences, Canberra, Australia.

Castro, J. J., Santiago, J. A., and Santana-Ortega, A. T. 2001. A general theory on fish aggregation to floating objects: An alternative to the meeting point hypothesis. Reviews in Fish Biology and Fisheries, 11: 255-277.

Collette, B. B., and Nauen, C. E. 1983. Scombrids of the world. An annotated and illustrated catalogue of tunas, mackerels, bonitos and related species known to date. FAO Fish Synop. 125(2). 137 pp.

Dagorn, L., Bez, N., Fauvel, T., and Walker, E. 2013a. How much do fish aggregating devices (FADs) modify the floating object environment in the ocean? Fisheries Oceanography, 22: 147-153.

Dagorn, L., Holland, K. N., Restrepo, V., and Moreno, G. 2013b. Is it good or bad to fish with FADs? What are the real impacts of the use of drifting FADs on pelagic marine ecosystems? Fish and Fisheries, 14: 391-415.

Désurmont, A., and Chapman, L. 2000. The use of anchored FADs in the area served by the Secretariat of the Pacific Community (SPC): regional synthesis. *In* Pêche thonière et dispositifs de concentration de poissons, Caribbean-Martinique, 15-19 Oct 1999 15-19 octobre 1999.

Ehrenberg, J. E., and Torkelson, T. C. 1996. Application of dual-beam and split-beam target tracking in fisheries acoustics. ICES Journal of Marine Science, 53: 329-334.

Eurocbc. 2015. Scottish Executive,Purse Seine Netting. http://www.eurocbc.org/page371.html.

FAO. 2012. Review of the state of world marine fishery resources 2011. Tuna and tuna-like species - Global, 2009. FIRMS Reports. In: Fishery Resources Monitoring System (FIRMS) [online]. Updated 28 June 2012. [Cited 20 January 2015].

Fonteneau, A., Ariz, J., Gaertner, D., Nordstrom, V., and Pallares, P. 2000a. Observed changes in the species composition of tuna schools in the Gulf of Guinea between 1981 and 1999, in relation with the Fish Aggregating Device fishery. Aquatic Living Resources, 13: 253-257.

Fonteneau, A., Palleres, P., and Pianet, R. 2000b. A worldwide review of purse seine fisheries on FADs. 20pp pp.

Foote, K., Knudsen, H., Vestnes, G., Maclennan, D., and Simmonds, E. 1987. Calibration of acoustic instruments for fish density estimation: a practical guide.

Foote, K. G. 1980. Importance of the swimbladder in acoustic scattering by fish: A comparison of gadoid and mackerel target strengths. The Journal of the Acoustical Society of America, 67: 2084-2089.

Forsbergh, E. D. 1980. Synopsis of Biological Data on the Skipjack Tuna.***Katsuwonus Pelamis*** (Linnaeus,1758) in the Pacific Ocean. . INTER-AMERICAN TROPICAL TUNA COMMISSION: 296.

Freon, P., and Misund, O. A. 1999. Dynamics of pelagic fish distribution and behaviour*,* Blackwell Fishing News Book, London.

Froese, R., and Pauly, D. 2014. http://www.fishbase.org. World Wide Web electronic publication.

García, S. M., Caddy;, J. F., Csirke;, J., Die;, D., Grainger, R., and Majkowski, J. 1994. World review of highly migratory species and straddling stocks. 70 pp.

Gerald, S. P., and Lopez, J. 2014. The use of FADS in Tuna Fisheries. Ed. by P. D. B. S. a. C. Policies. European Union: Directorate for Internal Policies: Fisheries.

Gooding, R. M., and Magnuson, J. J. 1967. Ecological significance of a drifting object to pelagic fishes. Pacific Science, 21: 486-487.

GoogleMap 2015. Map View. Accessed on 19th May,2015.

Graham, J. B., and Dickson, K. A. 2004. Tuna comparative physiology. Journal of Experimental Biology, 207: 4015-4024.

Hall, F. G. 1924. The functions of the swimbladder of fishes. The Biological Bulletin, 47: 79-[126]-121.

Hall, M., and Roman, M. 2013. Bycatch and non-tuna catch in the tropical tuna purse seine fisheries of the world.*,* FAO, Rome. 249 pp.

Hallier, J.-P., and Gaertner, D. 2008. Drifting fish aggregation devices could act as an ecological trap for tropical tuna species. Marine Ecology Progress Series, 353: 255-264.

ICCAT 2006. ICCAT Manual. 2014 edn. International Commission for the Conservation of Atlantic Tuna. In: ICCAT Publications [on-line]. http://www.iccat.int/en/ICCATManual.asp, ISBN (Electronic Edition): 978-92-990055-0-7. Retrieved September,2014.

ICCAT. 2008. Report of the Standing Committee on Research and Statistics (SCRS).29th September - 3rd October, 2008. Madrid, Spain.

ICCAT. 2012. Report of the Standing Committee on Research and Statistics (SCRS).1-5th October. Madrid, Spain.: PLE-104/2012.

ICCAT 2014a. Compendium of the management recommendations and resolutions adopted by ICCAT for the conservation of Atlantic tuna and tuna-like species.

ICCAT. 2014b. Report of the Standing Committee on Research and Statistics (SCRS).19th September-3rd October. Madrid, Spain.

IGFA 2001. Database of IGFA angling records until 2001. IGFA, Fort Lauderdale, USA.

Itano, D. 2012. What does a FAD look like, anyway? , 2nd May,2012 edn. International Seafood Sustainability Foundation.

IUCN 2014. IUCN Red List of threatened species, Downloaded on 16th November, 2014.

Jaquemet, S., Potier, M., and Ménard, F. 2011. Do drifting and anchored Fish Aggregating Devices (FADs) similarly influence tuna feeding habits? A case study from the western Indian Ocean. Fisheries Research, 107: 283-290.

Josse, E., Bertrand, A., and Dagorn, L. 1999. An acoustic approach to study tuna aggregated around fish aggregating devices in French Polynesia: methods and validation. Aquatic Living Resources, 12: 303-313.

Kailola, P., Williams, M., Stewart, P., Reicheit, R., McNee, A., and Grieve, C. 1993. Australian fisheries resources. Bureau of Resource Studies, Canberra.

Kuhn, W., Ramel, A., Kuhn, H. J., and Marti, E. 1963. The filling mechanism of the swimbladder. Experientia, 19: 497-511.

Lopez, J., Moreno, G., Sancristobal, I., and Murua, J. 2014. Evolution and current state of the technology of echo-sounder buoys used by Spanish tropical tuna purse seiners in the Atlantic, Indian and Pacific Oceans. Fisheries Research, 155: 127-137.

Lopez, J., Moreno, G., Soria, M., Cotel, P., and Dagorn, L. 2010. Remote discrimination of By-catch in purse seine fishery using fisher's echo-sounder buoys. ICES Document IOTC-2010-WPEB-03.

Love, R. H. 1977. Target strength of an individual fish at any aspect. The Journal of the Acoustical Society of America, 62: 1397-1403.

Lu, H.-J., Kang, M., Huang, H.-H., Lai, C.-C., and Wu, L.-J. 2011. Ex situ and in situ measurements of juvenile yellowfin tuna Thunnus albacares target strength. Fisheries Science, 77: 903-913.

Majkowski, J. 2007. Global fishery resources of tuna and tuna-like species, Food & Agriculture Org.

Majkowski, J. 2010. Tuna resources. FAO Fisheries and Aquaculture Department (Online), Rome.

Majkowski, J., and Goujon, M. 2000. Biological characteristics of tuna *In* FAO Fisheries and Aquaculture Department [online]. http://www.fao.org/fishery/topic/16082/en - StevensandNeill/1978, Rome [Date accessed :29th June, 2015].

Marsac, F., Fonteneau, A., and Ménard, F. 2000. Drifting FADs used in tuna fisheries: an ecological trap? *In* Pêche thonière et dispositifs de concentration de poissons, Caribbean-Martinique, 15-19 Oct 1999.

Matsumoto, T., Saito, H., and Miyabe, N. 2003. Report of observer program for Japanese tuna longline fishery in the Atlantic Ocean from September 2001 to March 2002. Col. Vol. Sci. Pap. ICCAT, 55: 1679-1718.

Maury, O. 2005. How to model the size-dependent vertical behaviour of bigeye (Thunnus obesus) tuna in its environment. Collect. Vol. Sci. Pap, ICCAT, 57: 115-126.

Miyake, M. P., Miyabe, N., and Nakano, H. 2004. Historical trends of tuna catches in the world.: No. 467. 74 pp.

Morgan, A. C. 2011. Fish Aggregating Devices and Tuna: Impacts and Management Options.

Nakken, O., and Olsen, K. 1977. Target strength measurements of fish. ICES.

Olsen, K. 1971. Orientation measurements of the cod in Lo- foten obtained from underwater photographs and their rela- tion to target strength. ICES CM, 1971/B:17: 8.

Ona, E. 1990. Physiological factors causing natural variations in acoustic target strength of fish. Journal of the Marine Biological Association of the United Kingdom, 70: 107-127.

Ona, E. 1999. Methodology for target strength measurements: with special reference to in situ techniques for fish and mikro-nekton. ICES Document CRR 235.

Ona, E., and Barange, M. 1999. Single target recognition. ICES Cooperative Research Report, 235: 28-43.

Ona, E., Foote, K. G., Zhao, X., and Svellingen, I. 1996. Some pitfalls of short-range standard-target calibration. ICES.

Pedersen, G., and Korneliussen, R. J. 2009. The relative frequency response derived from individually separated targets of northeast Arctic cod (Gadus morhua), saithe (Pollachius virens), and Norway pout (Trisopterus esmarkii). ICES Journal of Marine Science: Journal du Conseil, 66: 1149-1154.

Rudomiotkina, G. 1983. Areas, periods and conditions of bigeye tuna, Thunnus obesus (Lowe), spawning in the tropical part of the Atlantic Ocean. Collect. Vol. Sci. Pap, ICCAT, 18: 355-362.

Schaefer, M. B., Broadhead, G. C., and Orange, C. J. 1963. Synopsis on the Biology of Yellowfin Tuna (Pacific Ocean). ICES Document FIb/S59: Species synopsis No.16. 538-561 pp.

Sharp, G. D. 1978. Behavioral and physiological properties of tunas and their effects on vulnerability to fishing gear. The physiological ecology of tunas: 397-449.

Simmonds, E. J., and MacLennan, D. 2005. Fisheries acoustics: Theory and practice, Oxford. UK: Blackwell Scientific Publications.

SIMRAD 2006. ES10 Manual. Kongsberg Maritime AS. Document Reg. No.: 304120.

Stéquert, B., and Marsac, F. 1989. Tropical tuna: surface fisheries in the Indian Ocean. p. 238. FAO Fisheries Technical Paper, Rome.

Suzuki, Z. 1979. An aspect on catch of three major species, skipjack, Yellowfin and Bugeye tuna taken by the Japanese baitboat fleets based in Tema, 1969-78. ICCAT SCRS, 79.

Torgersen, T., and Kaartvedt, S. 2001. In situ swimming behaviour of individual mesopelagic fish studied by split-beam echo target tracking. ICES Journal of Marine Science: Journal du Conseil, 58: 346-354.

Warner, D. M., Rudstam, L. G., and Klumb, R. A. 2002. In Situ Target Strength of Alewives in Freshwater. Transactions of the American Fisheries Society, 131: 212-223.

Wittenberg, J. B. 1961. The Secretion of Oxygen into the Swim-bladder of Fish: I. The transport of molecular oxygen. The Journal of general physiology, 44: 521-526.

Zhao, X. 1996. Target strength of herring (Clupea harengus L.) measured by the split-beam tracking method. M. Phil. thesis, Department of Fisheries and Marine Biology, University of Bergen: 103 pp.

Websites

https://www.raspberrypi.org
https://www.arduino.cc

APPENDIX

APPENDIX A

Target direction determination and beam pattern compensation

The split beam transducer is electrically divided into four quadrants. During transmission, the four quadrants send signals or pulse simultaneously, upon reception however, each quadrant forms a separate beam. The sum of the four quadrants forms a full beam and two split beam sets.

The four separate signals are used to determine the target direction with the beam (α,β). α is the alongship angle and is determined by the sum of the fore-quadrant signals (FP+FS) and the sum of the aft-quadrant signals (AP+AS).

Also the athwartship angle (β) is also determined by the summed phase difference between the port and starboard (FP+AP and FS+ AS).

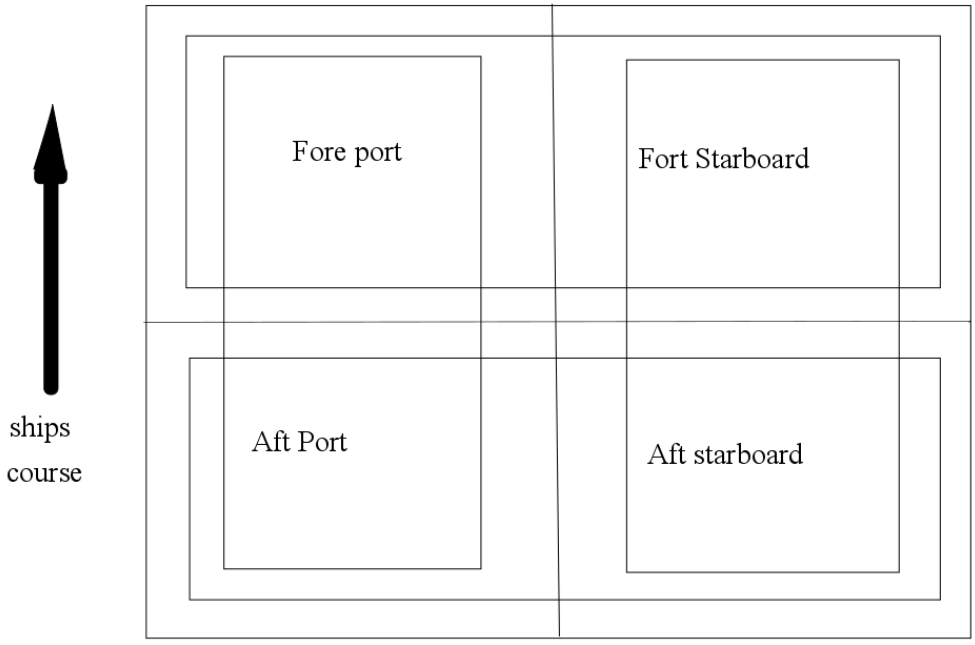

Figure 28. A schematic view of the four quadrants of the split beam with independent signal.

A target away from the transducer has an echo as a plane wave. For a wave (echo) from a target at an angle α relative to the transducer in the fore and aft plane of time

difference **Δ**t between the arrival of the echo from the fore and aft half of the quadrant are related by the equation

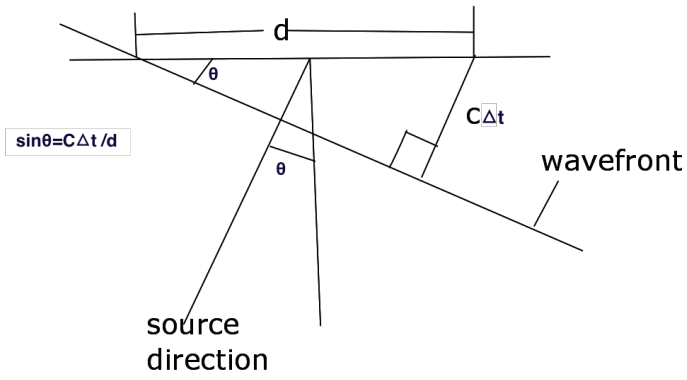

Fig. An illustration of angle of incidence of a wave arriving at two point sensors separated by distance d

$\sin\alpha = c*\Delta t/d$ -------**equation.1**

c is the sound speed, d is the effective distance between the fore and aft quadrants respectively.

The distance $c*\Delta t$ can be expressed in terms of path difference of the waves in terms of wavelength λ and phase difference $\delta(-\pi<\delta<\pi)$ as

$c*\Delta t=\delta*\lambda/2\pi=\delta/K$ -----**equation 2**

Where $k=2\pi/\lambda$ is the wave number

Since the angles are very small, the path difference is only a fraction of the wavelength.

Therefore

$\alpha=\sin^{-1}(\delta/Kd)$ ----------**equation 3**

The athwartship angle β is determined by the sum of the fore port and aft port (F.P + A.P) quadrant signals and the sum of the fore starboard and aft starboard signals (F.S + A. S).

When the exact location of the target within the beam is known, beam –pattern effect is then removed. In the Ek60 split beam echo sounder, the beam- pattern compensation is carried out by inserting the two angles (α, β) into the target strength measurements.

$TScomp=TSuncomp+2B(\alpha, \beta)$ ---------**equation 4**

Where TScomp and TSuncomp are beam-pattern target strength compensated and uncompensated target strength respectively and $2B(\alpha,\beta)$ is the two- way compensation.

APPENDIX B

Single echo acceptance criteria

Single echo detectors are implemented to ensure that only echoes originating from a single fish are accepted for further target strength analysis. This means the echoes must be far from other neighbouring echoes to avoid interference, and echoes from fish schools, bottom, noise, overlapping echoes from similar range and interferences are rejected.

A series of algorithm are implemented to filter the echoes and accept only valid candidates for target strength estimate. A typical single echo detector has the following algorithm

a. Target strength threshold filter

A minimum target strength threshold at the maximum directivity compensation B_{max} is set to exclude noise and unwanted weak echoes.

b. Pulse duration window

A minimum Pulse length filter is set to remove spikes, interference and maximum echo length filter to remove echoes from more than one fish occurring at similar range with overlapping echoes. The pulse duration window is set at -6dB relative to the peak amplitude. The echo must be within the minimum and maximum echo length filter. Also echoes too close in the vertical domain at the -6dB level are rejected to discriminate single from overlapping echoes.

c. Beam-pattern filter

The mean phase angles (α, β) are computed to determine the direct position of the target within the acoustic beam and thus compensated for in the echo amplitude.

d. Target separation filter

Adjacent echoes must be at least one pulse length apart.

e. Multiple peaks filter

When two peaks are detected within the pulse with a difference more than 0.5dB between the local maxima and the local minima, the echoes are rejected as multiple target echoes.

APPENDIX C

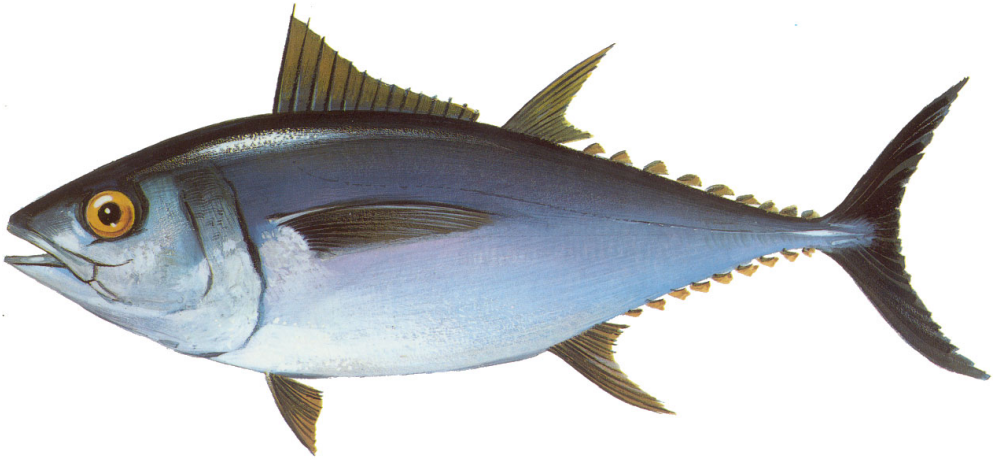

Figure 29. Bigeye tuna, *Thunnus obesus* (Lowe, 1839)

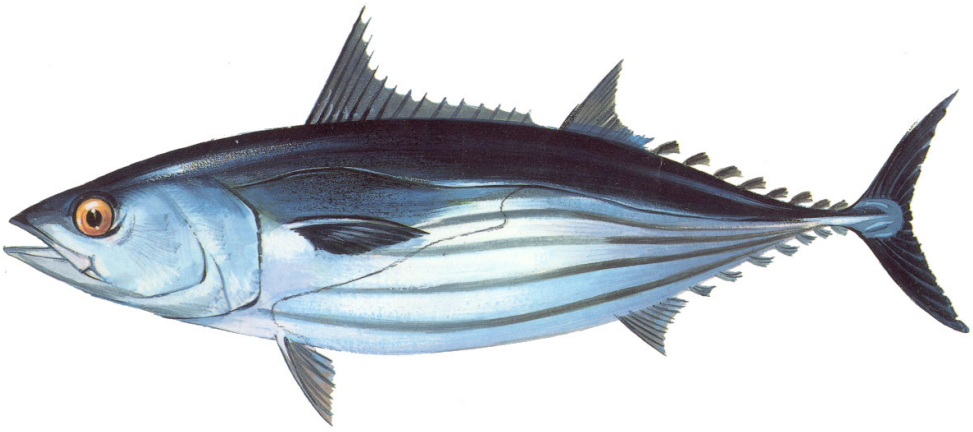

Figure 30. Skipjack tuna, *Katsuwonus pelamis* (Linnaeus, 1758)

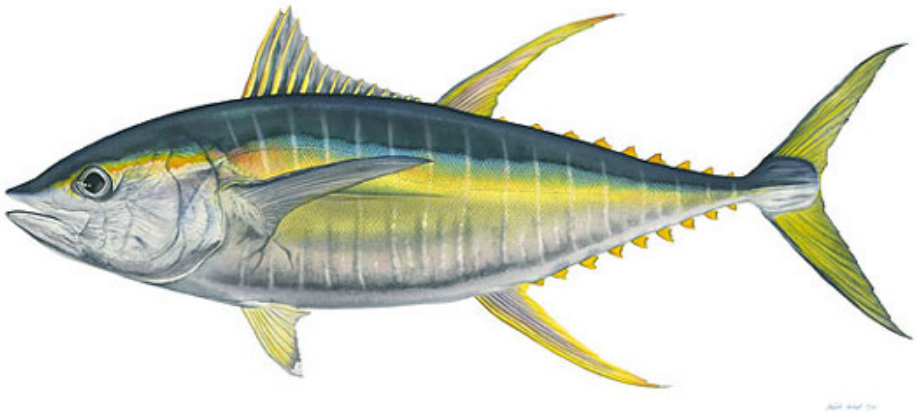

Figure 31. Yellowfin tuna, *Thunnus albacares* (Bonnaterre, 1788)

Figure 32. Atlantic cod, *Gadus morhua* (Linnaeus 1758).

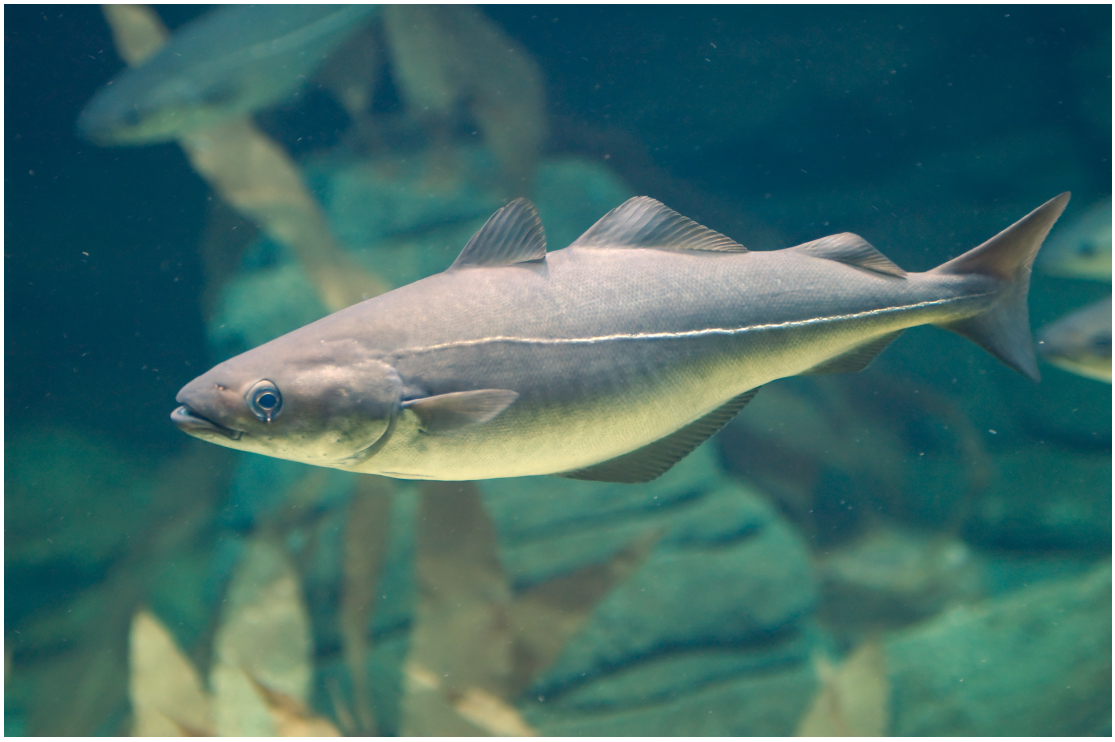

Figure 33. Saithe, *Pollachius virens* (Linnaeus 1758).

Source: (FAO, 2012; Froese and Pauly, 2014)

APPENDIX D
ALGORITHM AND OTHER ANALYSIS USED IN R

SINGLE BEAM ECHO SOUNDER DATA READING

#Reading ES10 data

>readES10=function(x,

 # Frequency for each ping

>freq=190476,

 # Sample interval duration for each ping:

>sint=21e-6,

#Pulse length

>plsl=0.000333,

 # Average speed of sound for each ping:

>asps=1488,

 # Absorption coefficient for each ping:

>absr=0.0102868,

 # Calibration factor

>cal=3.581386e-09

){

> dataES10=read.csv(x,header=FALSE)

>dataES10=t(as.matrix(dataES10))

> datetime=dataES10[1,]

>dataES10=dataES10[-1,]

 # sv for each ping

>vbsc=dataES10

 # Length of the beams:

>lenb=nrow(vbsc)

 # Create a list to input to the cplot2d.TSD function:

>dataES10=list(vbsc=vbsc*cal, sint=sint, asps=asps, freq=freq, lenb=lenb, absr=absr, plsl=plsl, asps=asps)

 # Get the TS:

```
>dataES10$sigmabs = add.TVG(dataES10$vbsc, dataES10, TVG.exp=2)
>dataES10
}
```

 # Read the ES10 test data:

```
>library(fields)
```

#Source functions

```
>fileListForSourcing = list.files("/Users/NewBeginnin/Dropbox/Thesis/Acoustics Thesis/  Data/ek60 in R/Functions for Data analysis.TSD",full.names=TRUE, recursive=TRUE)
>for(i in fileListForSourcing){
   source(i)
}
```

#source the ES10 calibrated data

```
>data=readES10("/Users/NewBeginnin/Desktop/Data from Austevoll4-6_12_2014/ES10Data/ES10Data20141204170304.txt",plsl=0.33e-3, sint=21e-6, cal=3.882867e-9)
```

 # plot a 2D echogram using the cplot2d.TSD function:

```
>cplot2d.TSD(data, breaks=seq(-60,-10),zlim=c(-1,-30),freq=190476, t=1:18000, var="sigmabs")
```

SPLIT BEAM ECHO SOUNDER DATA READING

#Import libraries

>library(fields)

>library(R.utils)

#Source functions

>sourceDirectory("/Users/NewBeginnin/Dropbox/Thesis/Acoustics Thesis/
Data/ek60 in R/Functions for Data analysis.TSD")

Use "readEKRaw" to read the EK60 raw data

> d=readEKRaw("/Users/NewBeginnin/Dropbox/Thesis/Acoustics Thesis/
Data/ek60 in R/cod raw files/Cod-D20030405-T093446.raw",t="all",drop=TRUE)

> d=readEKRaw_power2sv(d)

 # Frequency for each ping

>freq=d$data$config$frequency

 # Sample interval duration for each ping:

>sint=d$data$pings$sampleinterval[seq_along(freq)]

 # Sample interval duration for each ping:

>plsl=d$data$pings$pulselength[seq_along(freq)]

 # Average speed of sound for each ping:

>asps=d$data$pings$soundvelocity[seq_along(freq)]

 # Absorption coefficient for each ping:

>absr=d$data$pings$absorptioncoefficient[seq_along(freq)]

 # sv for each ping:

>vbsc=d$data$pings$sv

 # Length of the beams:

lenb=nrow(vbsc)

 # Create a list to input to the cplot2d.TSD funciton:

#data=list(vbsc=vbsc,plsl=plsl,sint=sint/4,asps=asps,freq=freq,lenb=lenb,absr=absr)

>data=list(vbsc=vbsc,plsl=plsl,sint=sint,asps=asps,freq=freq,lenb=lenb,absr=absr)

 # Get the TS:

>data$sigmabs = add.TVG(data$vbsc,data,TVG.exp=4)

 # Add TVG:#ITS 20log R without #TVG.exp=4 thus TS with 40log R

>data$vbsc=add.TVG(data$vbsc,data)

 # A 2D echogram:

>cplot2d.TSD(data, breaks=seq(-82,-30),zlim=c(-0,-100), freq=38000, t=3319:3319)

SINGLE ECHO DETECTION (SED)

SED FUNTION

```
singleTargetDetection <- function(data, t=100, TSmin=-55, TSmax =-20, wb=5, ws=6,
insertNA=TRUE, nearField=1:20, noise.add=20, clean=FALSE, range=NULL){
  # Subset the data:
  data$sigmabs = data$sigmabs[,t, drop=FALSE]
  # Select the range specified by 'range':
  pulselength = data$asps*data$sint / 2
  if(length(range)==2){
    range=abs(range)
    data$sigmabs[seq_len(floor(range[1]/pulselength)),] = NA
    data$sigmabs[seq(ceiling(range[2]/pulselength),nrow(data$sigmabs)),] = NA
  }
  #Threshold TSmin#1
  if(clean){
    data$sigmabs = CleanSv(data$sigmabs, wb=wb, ws=ws, insertNA=insertNA,
nearField=nearField, noise.add=noise.add)
  }
  Npings=ncol(data$sigmabs)
  # Get the effective pulselengths between 50 and 150 % of the pulselength in
units of sample intervals:
  if(length(data$plsl)==0 || length(data$sint)==0){
  stop("Pulseduration and sample interval duration must be present in 'data'")
  }
  validpulselengths = data$plsl/data$sint * c(0.5,1.5)
  singletargets = rep(list(list()),Npings)
  singletargetsEffBW = singletargets
  singletargetsMeanTS = singletargets
  for(j in seq_len(Npings)){
    TS = 10*log10(data$sigmabs[,j])
    # Single target candidates:
    valid=rep(TRUE,length(TS))
    valid[is.na(TS)]=FALSE
    # Step 1:
```

```
      valid = valid & TS>TSmin & TS<TSmax
      #step 2:
      cand=which(valid)
      if(length(cand)>0){
      # Get the starting points of unbroken sequences of cod-values:
        starts=which(c(2,diff(cand))>1)
      # Get the end points of unbroken sequences of cod-values:
        ends=which(c(diff(cand),2)>1)
      # Get the lengths of the cod candidates:
        lengths=ends-starts+1
      # Get the effective lengths of the cod candidates:
        effBW = double(length(ends))
        for(i in seq_along(ends)){
          thiscand=cand[starts[i]]:cand[ends[i]]
          TStarg = 10^(data$sigmabs[thiscand,j]/10)
       # Apply the -6 dB: to the Peak amplitude.
          above6=TStarg > max(TStarg) * 10^(-6/10)
          thiscand = thiscand[above6]
          TStarg = TStarg[above6]
          effBW[i] = sum(TStarg)/max(TStarg)
       # Pick out the accepted candidates:
          if(isTRUE(effBW[i] >= validpulselengths[1]) && isTRUE(effBW[i] <=
validpulselengths[2])){
            singletargets[[j]] = c(singletargets[[j]], list(thiscand))
            singletargetsEffBW[[j]] = c(singletargetsEffBW[[j]], list(effBW[i]))
            singletargetsMeanTS[[j]] = c(singletargetsMeanTS[[j]],
10*log10(mean(TStarg,na.rm=TRUE)))
          }
        }
      }
    }
    list(targ=singletargets, effBW=singletargetsEffBW,
meanTS=singletargetsMeanTS)
}
```

```
  Where; t= number of pings, TS max, TS min are the TS threshold.
################## Sourcing the SED function ###########
  st = singleTargetDetection(data, t=1:3319, TSmin=-55, TSmax =-20, wb=5, ws=6,
  insertNA=TRUE, nearField=1:20, noise.add=20, range=c(50,65))
  singletargets = st$targ
  singletargetsEffBW = st$effBW
  singletargetsMeanTS = st$meanTS

  for(i in seq_along(singletargets)){
     for(j in seq_along(singletargets[[i]])){
        l=length(singletargets[[i]][[j]])
        points(rep(i,l), -singletargets[[i]][[j]] * (data$asps*data$sint/2),pch=".")
     }
  }
  sapply(singletargets,length)
  numtargets=sapply(singletargets,length)
  pingswithtarget= which(numtargets>0 & numtargets < 5)
  pingswithtarget
  singletargetsMeanTS[pingswithtarget]
```

SINGLE TARGET TRACKING

############### TARGET TRACKING ########################

```
trackST = function(st, MAXPINGDIFF=2, MAXRANGEDIFF=2,
MINPINGSPAN=8, list.out=FALSE){
   # Clean away empty pings:
   stTargCleaned = unlist(st$targ, recursive=FALSE)
   # Get single target IDs:
   stID = seq_along(stTargCleaned)
   # Get ping IDs:
   numtargetsInPing = sapply(st$targ,length)
   pingID = which(numtargetsInPing>0)
   numtargetsInPing = numtargetsInPing[pingID]
   pingID = rep(pingID, numtargetsInPing)
   # Move through the single targets and merge to tracks:
   tracks = list()
   trackPings = list()
   trackStep = 0
   finished = FALSE
   while(!finished){
      # The current track ID:
      initialST = head(stID[!is.na(stID)], 1)
      currentST = initialST
      # If there are any current tracks left:
      if(length(initialST)){
      # Remove the current single target (which is the first single target of the
track):
         stID[initialST] = NA
       # Move to the next track ID:
         trackStep = trackStep + 1
         thisfinished = FALSE
         tracks[[trackStep]] = list()
         # Move through the available single targets:
```

```
        stStep = 0
        # Get the ID if the current available single target:
        availableST = stID[!is.na(stID)]
        NavailableST = length(availableST)
        if(length(availableST)){
          availableInd = 1
          while(!thisfinished){
            if(NavailableST<availableInd){
              break
            }
            currentAvailableST = availableST[availableInd]
            # 1. Check whether the single target is close enough in time:
            pingdiff = pingID[currentAvailableST] - pingID[currentST]
            withinPingLimit = pingdiff <= MAXPINGDIFF
            # 2. Check whether the single target is close enough in range:
            L = min(stTargCleaned[[currentST]]) - MAXRANGEDIFF
            H = max(stTargCleaned[[currentST]]) + MAXRANGEDIFF
            withinRangeLimit = any(stTargCleaned[[currentAvailableST]] >= L &
stTargCleaned[[currentAvailableST]] <= H)
            # This is an accepted candidate:
            if(withinPingLimit && withinRangeLimit){
              stStep = stStep + 1
              tracks[[trackStep]][[stStep]] = stTargCleaned[[currentAvailableST]]
              names(tracks[[trackStep]])[stStep] = pingID[currentAvailableST]
              currentST = currentAvailableST
              # Remove the current available single target:
              stID[currentAvailableST] = NA
            }
            else if(pingdiff>MAXPINGDIFF){
              thisfinished = TRUE
            }
            availableInd = availableInd+1
          }
        }
```

```
            else{
                finished = TRUE
            }
        }
        else{
            finished = TRUE
        }
    }

    # 3. Remove merged detections over less than MINPINGSPAN:
    tracks= tracks[sapply(tracks,length)>=MINPINGSPAN]
    # Return a matrix as default:
    if(!list.out){
        tracks = lapply(tracks, function(x) cbind(unlist(x), rep(as.numeric(names(x)),
sapply(x,length))))
    }
    # Return:
    tracks
}
test = trackST(st, MAXRANGEDIFF=3,MAXPINGDIFF=3, MINPINGSPAN = 8)
```

############ END OF TRACK ################

MAKING PLOTS FOR TRACKED AND UNTRACKED TS DISTRIBUTION UNTRACKED

```
##################### UNTRACKED TS FOR TS DISTRIBUTION  ###
#Backscattering cross - section of single echoes
TSlin= (unlist(singletargetsMeanTS[pingswithtarget]))
#Converting into TS
TSmean=10*log10(TSlin)
#Distribution of single targets TS
hist((TSmean),breaks=35,xlab="TS (dB)",ylab="Count",main="")
#sd of distribution
SD=sd(TSmean)
#mean of distribution in linear domain
meanTS=10*log10(mean(unlist(TSlin)))
#counts of number of detections
N=length(unique(TSmean))
#adding mean TS, SD and N as texts to the graph
text(-25, 600, paste("TS =", round(meanTS, 1), "\n N =",round(N, 1), "\n Std.Dev =",
round(SD, 2)))
#Indicating the mean on the plot
abline(v=meanTS, col = 2)
#box around the graph
box(lwd=1)

##### 95% CONFIDENCE INTERVAL ~ 0.05 ######
error <- qnorm(0.975)*SD/sqrt(N)
error



############ TRACKED TS DISTRIBUTION #########
tracksdata = lapply(test, function(x) data$sigmabs[x])
# backscattering cross – section of tracked single targets
TSlinTrk= lapply(tracksdata,mean)
#TS of tracked single targets
```

```
TSmeantrk=10*log10 (unlist(TSlinTrk))
#Distribution of single tracked targets TS
hist((TSmeantrk),breaks=33,xlab="TS (dB)",ylab="Count",main="TS distribution of
tracked fish")
#sd of distribution
SD=sd(TSmeantrk)
#mean of distribution
meanTS=10*log10(mean(unlist(TSlinTrk)))
#counts of number of targets
N=length(unique(TSmeantrk))
#adding mean TS, SD and N as texts to the graph
text(-41, 29, paste("TS =", round(meanTS, 1), "\n N =",
round(N, 1), "\n Std.Dev =", round(SD, 2)))
#Indicating the mean
abline(v=meanTS,col=2)
# A box around the graph
box(lwd=1)

##### 95% CONFIDENCE INTERVAL ~ 0.05 ######
#percentage confidence interval = z = (aplha/2)
#alpha=percentage of error, thus at 95 %, 5 % error ~5/100 = 0.05
#at 95%, alpha = 0.10, at 95% alpha = 0.05.z = 0.025
error <- qnorm(0.975)*(SD/sqrt(N))
error

################ TS – LENGTH OF FISH RELATIONSHIP PLOTS
TS = 20*LOG10 (L) – 68 -------equation of TS – fish length

LengthFish=10^((TSmean+68)/20)
#Fitting a linear model
lmfit = lm(TSmean ~ LengthFish) # create a model for the x, y values
#A plot of the TS – fish length
plot(TSmean~LengthFish,axes= F,type="n",xlim=c(min(x),150), ylab="TS
(dB)",xlab ="Length (cm)") # plot x, y
```

 # Apply the fitted model

```
abline (lmfit, col=2) # fit the model to the plot
axis(2, las=1) # y axis label
axis(1, las=1) # x axs label
box()

################################### TS - log10 length #########
LengthFish=10^((TSmean+68)/20)

lmfit=lm(TSmean~log10(LengthFish)) # create a model for the x, y values
plot(TSmean~log10(LengthFish),axes = F,type="n", ylab="TS (dB)",xlab ="Log10
Length(cm)") # plot x, y
abline(lmfit,col=2) # fit the model to the plot
axis(2, las=1) # y axis label
axis(1, las=1) # x axs label
box()
```

####### PLOTTING THE CTD PROFILE

#Import file

```
soundV<-read.delim(file.choose(),header=T)
# Attach file
attach (soundV)
soundV
```

#set the dimensions for graph

```
par(mar=c(5,5,8,4)+0.01)
```

#plot Pressure Vrs Sound velocity

```
#Depth<-as.factor(Press)
#Depth<-factor(Press,levels=rev(levels(Press)))
plot(Press~Speed.Water.,ylab="Depth
(m)",ylim=c(max(Press),min(Press)),xlab="sound velocity
(m/s)",type="l",lty=1,col=2)
#points(Press,Speed.Water.,pch=20,col=4)
#axis(3,ylim=c(0,max(Speed.Water.)),line=1,col=)
#mtext(side = 1,ylab="sound velocity", text="sound velocity",line=1)
```

 # Adding a new plot

```
#par(new=T)
#plot Pressure Vrs Temperature
#plot(Press~Temp,axes=F,ylim=c(10,max(Temp)),type="l",lty=2,col=2)
#points(Press,Temp,pch=20)
#axis(3,ylim=c(0,max(Temp)),line=3)
#mtext(side = 3,text="Temperature",line=3)
# Adding a new plot
par(new=T)
#Plot Pressure Vrs Salinity
plot(Press~Sal.,axes=F,type="l",ylim=c(max(Press),min(Press)),ylab="Depth(m)",xla
b=rm,lty=3,col=3)#ylim = rev(range(x))
#points(Press,Sal.,pch=20)
axis(3,ylim=c(0,max(Sal.)),line=0)
mtext(side = 3,text="Salinity (psu)",line=2)
#plotting the x-axis
axis(1,pretty(range(1.0,max(Press)),10))
#mtext("Pressure",side=1,col=1,line=3)
# Add legend
legend("bottomleft",inset=0.05,legend=c("Sound
velocity","Salinity"),lty=c(2,3),col=c("2","3"))
#adding a line to indicate the point of where the Sound velocity was used
abline(h=5,lty=1).
```